"Developing DILI models in zebrafish for screening of hepatoprotective agents"

Dissertation submitted to

In partial fulfilment of the requirements of the BS-MS dual degree programme, IISER Pune

By

Lavanya Lokhande

(Reg. No. 20161060)

Under the guidance of

Dr. Chetana Sachidanandan

Senior Scientist

CSIR-Institute of Genomics and Integrative Biology (IGIB), New Delhi

CERTIFICATE

This is to certify that this dissertation entitled "***Developing DILI models in zebrafish for screening of hepatoprotective agents***" towards the partial fulfilment of the BS-MS dual degree programme at the Indian Institute of Science Education and Research, Pune represents study/work carried out by **Lavanya Lokhande**, roll no. – **20121060** at **CSIR-Institute of Genomics and Integrative Biology (IGIB), New Delhi**, under the supervision of **Dr. Chetana Sachidanandan**, Senior Scientist, Zebrafish Chemical Genetics Laboratory, Department of Chemical and Systems Biology, during the academic year May 2016-March 2017.

Dr. Chetana Sachidanandan
(Supervisor, Senior Scientist,
CSIR-IGIB, New Delhi)

Lavanya Lokhande
BS MS Student,
IISER Pune

Date: 17th MARCH 2017

Place: NEW DELHI

DECLARATION

I hereby declare that the matter embodied in the report entitled "***Developing DILI models in zebrafish for screening of hepatoprotective agents***" are the results of the work carried out by me at the Zebrafish Chemical Genetics Laboratory, Department of Chemical and Systems Biology, CSIR-Institute of Genomics and Integrative Biology (IGIB), New Delhi, under the supervision of **Dr. Chetana Sachidanandan** and the same has not been submitted elsewhere for any other degree.

Dr. Chetana Sachidanandan
(Supervisor, Senior Scientist,
CSIR-IGIB, New Delhi)

Lavanya Lokhande
BS MS Student,
IISER Pune

Date: 17th MARCH 2017

Place: NEW DELHI

CONTENTS

Abstract ---------- *5*

List of Figures ---------- *6*

List of Tables ---------- *6*

Acknowledgements ---------- *7*

1. Introduction ---------- 8
2. Materials and methods ---------- 18
3. Results ---------- 27
4. Discussion ---------- 44
5. References ---------- 47

ABSTRACT

Drug Induced Liver injury (DILI) is one of the causes of liver failure. In severe conditions, treatment for DILI is limited to liver transplant. Therefore, there is an urgent need for therapeutics that may counter DILI. *Danio rerio*, commonly known as zebrafish has emerged as a popular vertebrate model for drug screening. Using zebrafish, as a model system, we have successfully developed embryonic and adult zebrafish DILI models using acetaminophen (APAP) and Isoniazid (INH). Acetaminophen (paracetamol) is a known hepatotoxic molecule, extensively studied in multiple model systems and has become one of the major causes of acute liver failure. Isoniazid is a drug prescribed for Tuberculosis (TB). Since, TB is highly prevalent in India; hepatotoxicity due to INH has become a serious issue in the Indian sub-continent. Using *fabp10a* as a marker for liver, we have shown by multiple means that both drugs down-regulate the expression of *fabp10a* thus indicating damage. Other techniques were used to characterize both the DILI models and study their post-damage effects. Using the INH-induced liver-damage model, we have screened 15 small molecules for their hepatoprotective effect and have found one molecule as a potential candidate. These models can be used for further screening of novel small molecules and enable us to understand DILI as well as the mechanisms of small molecules that can revert it.

LIST OF FIGURES

Figure 1: Pictorial representation of different stages of liver damage and the cause of injury. Figure taken from Pellicoro et al., 2014.

Figure 2: The different mechanism of the drug metabolism in the liver. Image taken from Almazroo et al., 2017.

Figure 3:3-step mechanistic model of hepatotoxicity. Figure adapted from Russmann et al., 2009.

Figure 4: Mechanism of acetaminophen mediated hepatotoxicity.

Figure 5: Mechanism of Isoniazid mediated hepatotoxicity.

Figure 6: Schematic and pictorial representations of mammalian and zebrafish liver architecture. The figure is taken from Vliegenthart et al., 2014.

Figure 7: Hepatotoxicity with APAP.

Figure 8: Hepatotoxicity with INH.

Figure 9: Assessment of hepatotoxicity due to APAP and INH using transgenic line Tg(*fabp10a:Gal4-VP16, my17:cerulean*).

Figure 10: DCFDA Assay INH and APAP

Figure 11: Characterization of APAP Damage

Figure 12: Characterization of INH Damage

Figure 13: Developmental defects post APAP damage

Figure 14: Developmental defects post INH damage

Figure 15: In-situ hybridization quantification of embryos co-treated with INH 7.5mM and CSLR001

LIST OF TABLES

Table 1: Table summarizes the different phenotypes of liver damage. Table adapted from William M, 2003.

ACKNOWLEDGEMENTS

First and foremost, I would like to express my deep gratitude towards Dr. Chetana Sachidanandan for giving me an opportunity to work in her lab and gain this wonderful learning experience. I am also thankful for all her encouragement, enthusiasm and guidance.

I would like to thank Urmila Jagtap for being an incredible mentor, for teaching me and assisting me throughout the course of the project. And more importantly boosting my morale and providing me with encouragement whenever necessary.

I would also like to acknowledge Nikhil Bharti and Sandeep Basu. Their assistance and helpful insights were pivotal for the completion of this project.

I am thankful to all my lab mates for their tremendous knowledge and assistance whenever I needed their help.

I also want to thank Prof. LS Shashidhara, my TAC member from IISER Pune for being my guide.

A special thanks to CSIR-IGIB for providing me infrastructure and facilities necessary for the completion of this project.

1. INTRODUCTION –

The human body has approximately 79 organs out of which liver is among the very few organs which can regenerate. It carries out multiple functions which include energy metabolism, nutrient processing and storage, detoxification of xenobiotics, RBC decomposition, fat metabolism, synthesis of bile and hormones like angiotensin, IGF1 etc. (Hong and Tontonoz, 2014; Ko et al., 2010a; Nguyen et al., 2008; Rui, 2014; The liver - Canadian Cancer Society). The functions that liver carries out towards rest of the body are so essential, that any loss towards maintaining these functions can have detrimental effects on the organism. This might be why evolution has ensured that liver has the immense ability to regenerate in order to protect it from variety of insults. It has been proven that liver can completely restore back to its original size and function even after 75% of its mass has been surgically removed (Fausto et al., 1995; Michalopoulos, 1990). This capacity however is not omnipotent. In spite of this immense capacity to survive damage, the number of people suffering from liver diseases has been found to be steadily increasing over the decades. In 2013, nearly 30 million Americans suffered from some form of liver disease (The International Liver Congress, 2016). In India, liver disease claim nearly 2.44% of all the deaths (Liver Disease in India). This statistics suggests that the liver's capacity to cope up with the stress is affected in certain type of insults. A failure in regenerating capacity of liver has found in variety of diseases like hepatitis, fibrosis, cirrhosis, hepatocellular carcinoma etc. If not treated, many of these can be fatal. The underlined causes for these include bad lifestyle, hepatitis virus, alcohol abuse and excessive drug intake etc. (Ko et al., 2010b). Currently, we do not have many remedies or other drugs to counteract these liver injuries, except liver transplant, in extreme cases. Hence, there is an urgent requirement in the market for potential therapeutic remedies to combat various kinds of liver damages. Multiple studies have been done towards finding the causes of liver damage. In this study, our interest is to study Drug Induced Liver Injury (DILI).

1.1 DRUG INDUCED LIVER INJURY (DILI)

Over the past few decades, the number and different types of drugs in market have risen exponentially and so has the incidence rate for Drug Induced Liver Injury (DILI). DILI is one of the leading causes of acute liver failure in United States (Au et al.,

2011; Suk et al., 2012). As liver is the primary organ for xenobiotic and drug metabolism, it becomes vulnerable to damage by any toxic product that may be formed during the course of treatment of other organs. Many commonly used and commercially available drugs have been proven to be hepatotoxic. Examples of these include Isoniazid and Rifampicin (TB drugs), Sertraline, NSAIDs, HAART drugs, Omeprazole, Statins etc. (Bessone, 2010; Mahadevan et al., 2006; Navarro and Senior, 2006; Tostmann et al., 2008). Drugs like these have further affected the pharmaceutical companies as most drugs are not approved by the FDA because of their hepatotoxic side effects (Au et al., 2011). As the natural response of liver towards the toxicity i.e. regeneration is compromised in DILI, we intend to identify potential small molecule therapeutics that may promote liver regeneration in this background. Using zebrafish, as a model system, we have developed and characterized two DILI models using Acetaminophen (APAP) and Isoniazid (INH) and have used these models to screen for liver regenerative compounds.

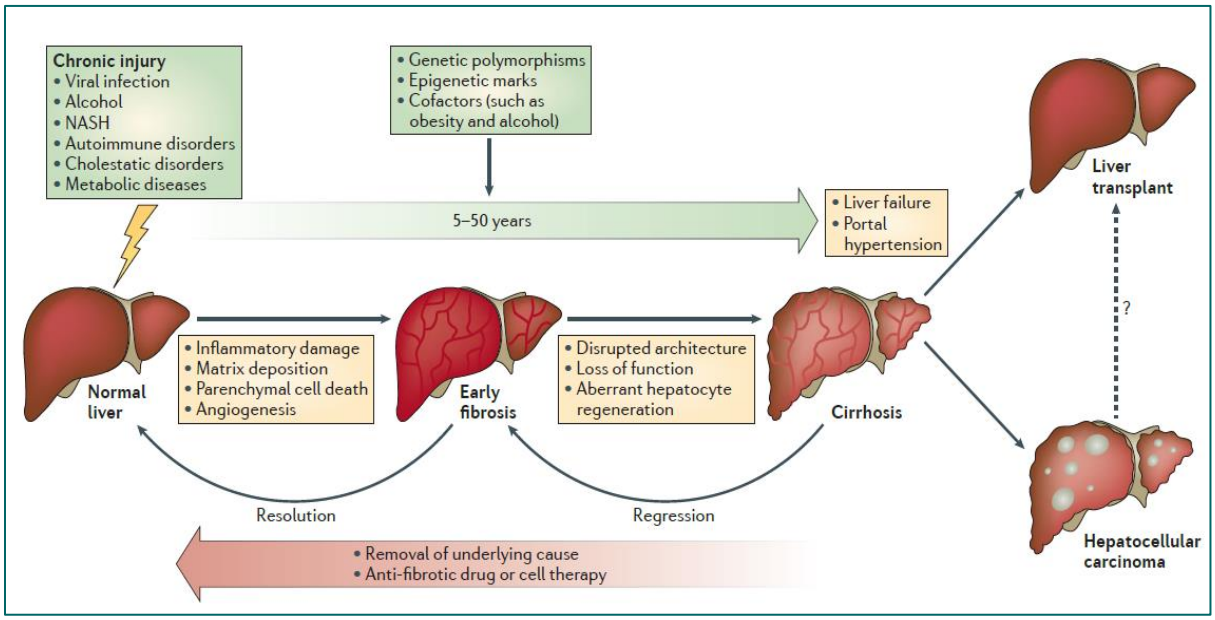

Figure 1: *Figure demonstrates how liver damage occurs due to multiple reasons such as viral infection, drugs, alcohol etc. This causes fibrosis and can further leads to liver failure. Figure taken from Pellicoro et al., 2014.*

1.2 DRUG METABOLISM IN LIVER-

The general mechanism of drug metabolism can be summarised in 3 phases –

1.2.1 Phase 1: Modification –

This phase involves various modifications like addition of thiol, hydroxyl, carboxyl groups etc. on the parent drugs in order to make them more hydrophilic. This is majorly performed by the action of CYP450 superfamily of enzymes (Corsini and Bortolini, 2013). In human liver, CYP3A4, CYP2E1 and CYP2C9 are the most abundant enzymes involved in this process(Almazroo et al., 2017).

1.2.2 Phase 2: Conjugation –

The products formed by phase 1 modification are further conjugated with endogenous molecules such as glutathione (GSH), acetates, sulfate, glucuronic acid etc. (Almazroo et al., 2017). Several enzymes are involved in the catalysis of such reactions depending upon the type of conjugation. These enzymes include uridinediphosphateglucuronosyltransferase (UGT), N-acetyltransferase 2 (NAT2), and glutathione S-transferase (GST) (Corsini and Bortolini, 2013).

1.2.3 Phase 3: Transportation –

The last phase of detoxification involves transportation of the metabolites out of the cell. It is carried out with the help of transmembrane proteins majorly belonging to these superfamilies – ATP-binding cassette (ABC) and solute carrier (SLC) transporters (Almazroo et al., 2017).

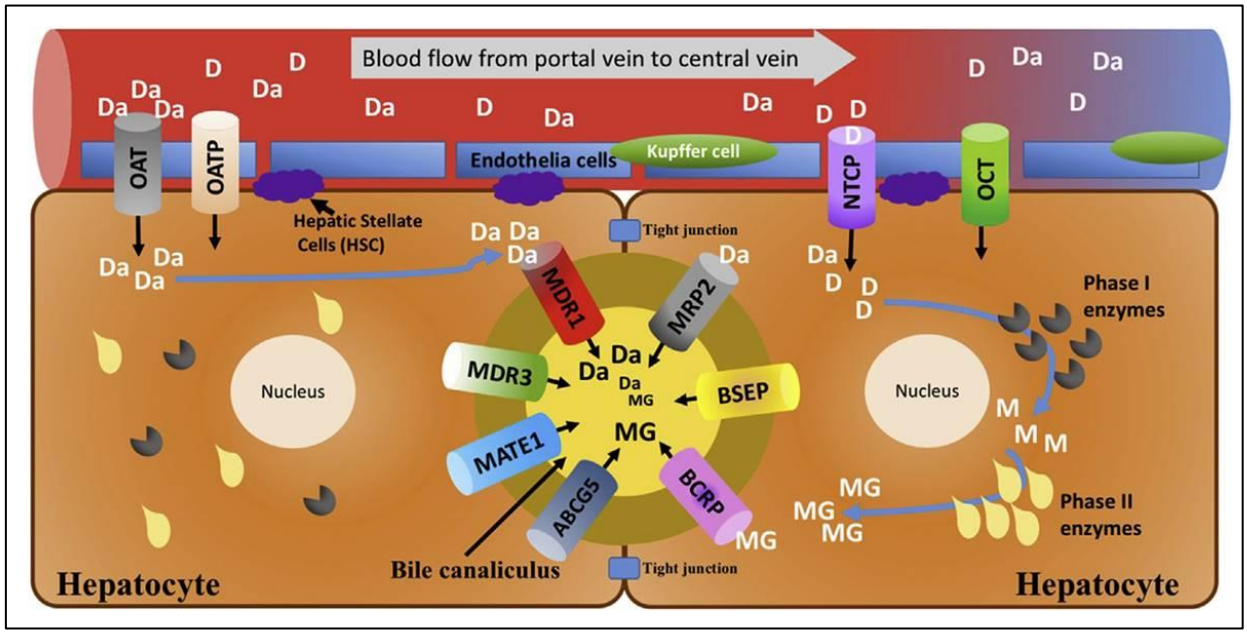

Figure 2: *The different mechanism of drug metabolism in liver of 2 drugs 'D' and 'Da'. 'D' is taken up by transporters and modified by phase1and then conjugated by phase 2 enzymes respectively. This is*

followed by removal by transporters into the biliary system. For drug 'Da', unlike 'D' there is no modification. It is taken in by influx OAT transporters and directly pumped out into the biliary system by efflux MDR transporters. Image taken from Almazroo et al., 2017.

1.3 MECHANISM OF DRUG INDUCED LIVER INJURY

The mechanism of drug induced liver injury can be summarised by a 3-step model -

1.3.1 Initial mechanism of toxicity

Though the purpose of modifications of the parent drug is to reduce its toxicity, the intermediates that are formed during this process are many a times equivalent or more reactive than the parent molecule. Both parent drug and intermediate drug-metabolite can cause the cell toxicity by inducing stress, mitochondrial dysfunction and inducing specific immune reactions. Cell stress can occur in multiple ways – by free radical formation, depletion of antioxidants like GSH, blocking of efflux transporters thus leading to intracellular accumulation of toxins (Russmann et al., 2009). This further can lead to damage to intracellular organelles like mitochondria (Russmann et al., 2009). Immune response by increase in inflammatory cytokines is often observed in drug toxicity

1.3.2 Mitochondrial Permeability Transition (MPT)

The initial reaction of cell stress and other immune reactions can lead to MPT i.e. formation of pores spanning both the mitochondrial membranes causing the loss of membrane potential. The drugs may cause the direct binding to mitochondrial DNA and lead to its damage. Drug/drug metabolites can also cause inhibition of respiratory chain and therefore ATP depletion, further causing inhibition of β-oxidation. If the injury is not recoverable, the mitochondrial permeability transition (MPT) can lead to induction of pro-apoptotic factors and result into cell death (Yuan and Kaplowitz, 2013).

1.3.3 Apoptosis and Necrosis

Cell death as a result of liver damage is a context dependent phenomenon i.e. depending on the level of ATP, the fate of the damaged cell is decided. In presence of critical levels of ATP, the cell undergoes apoptosis and in its complete absence, necrosis. However, it is difficult to distinguish between the two as both processes take place in a damaged tissue.

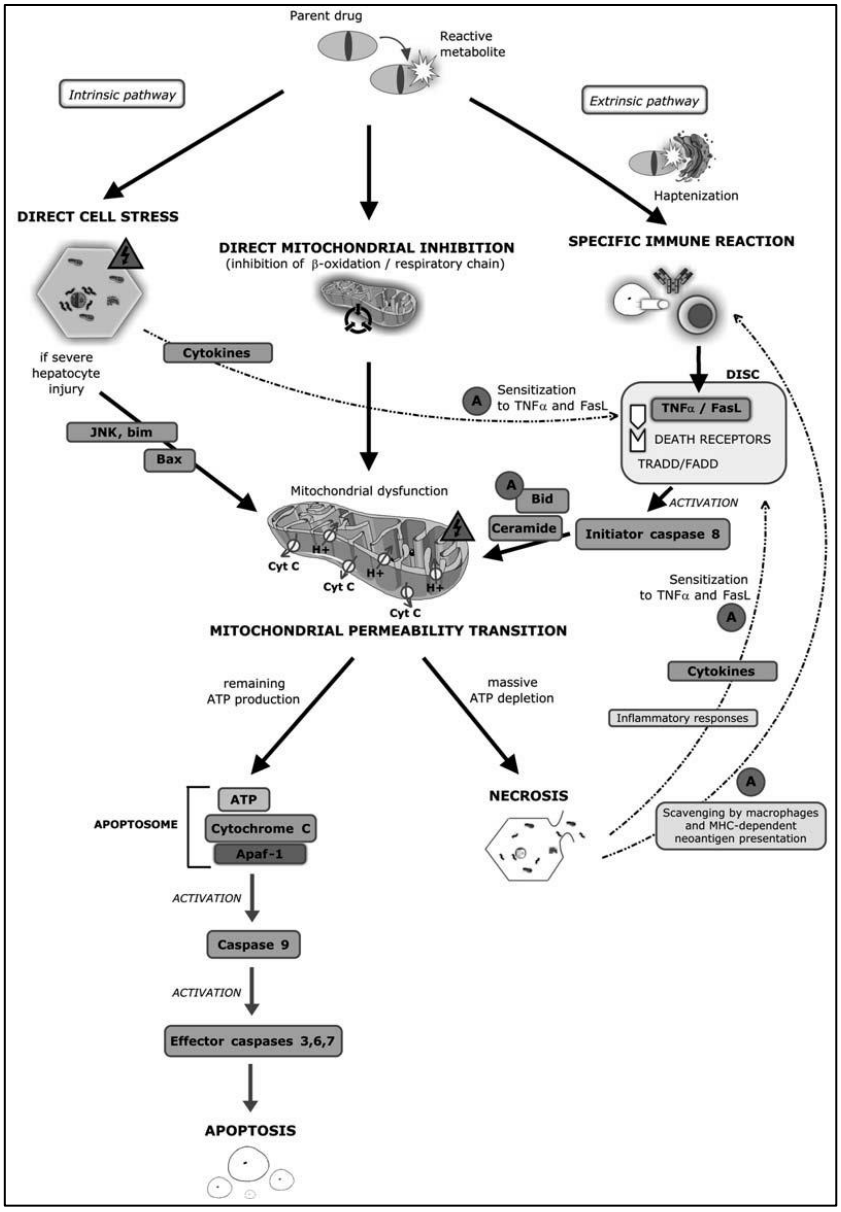

Figure 3:*3-step mechanistic model of hepatotoxicity. Figure adapted from Russmann et al., 2009.*

Depending on the nature of the drug, a variety of downstream mechanisms are followed leading to different pathophysiological phenotypes. A list of such reactions along with the drugs causing them and their respective effects on cells is given in the table below.

Type of Reaction	Effect on Cells	Examples of Drugs
Hepatocellular	Direct effect or production by enzyme–drug adduct leads to cell dysfunction, membrane dysfunction, cytotoxic T-cell response	Isoniazid, trazodone, diclofenac, nefazodone, venlafaxine, lovastatin
Cholestasis	Injury to canalicular membrane and transporters	Chlorpromazine, estrogen, erythromycin and its derivatives
Immunoallergic	Enzyme–drug adducts on cell surface induce IgE response	Halothane, phenytoin, sulfamethoxazole
Granulomatous	Macrophages, lymphocytes infiltrate hepatic lobule	Diltiazem, sulfa drugs, quinidine
Microvesicular fat	Altered mitochondrial respiration, β-oxidation leads to lactic acidosis and triglyceride accumulation	Didanosine, tetracycline, acetylsalicylic acid, valproic acid
Steatohepatitis	Multifactorial	Amiodarone, tamoxifen
Autoimmune	Cytotoxic lymphocyte response directed at hepatocyte membrane components	Nitrofurantoin, methyldopa, lovastatin, minocycline
Fibrosis	Activation of stellate cells	Methotrexate, excess vitamin A
Vascular collapse	Causes ischemic or hypoxic injury	Nicotinic acid, cocaine, methylenedioxymethamphetamine
Oncogenesis	Encourages tumor formation	Oral contraceptives, androgens
Mixed	Cytoplasmic and canalicular injury, direct damage to bile ducts	Amoxicillin–clavulanate, carbamazepine, herbs, cyclosporine, methimazole, troglitazone

Table 1: *Table summarizes the different phenotypes of liver damage. Table adapted from William M, 2003.*

As discussed previously, our objective is to screen for hepatoprotective molecule in the background of DILI. Towards this objective, we have used two potential drugs i.e. Acetaminophen and Isoniazid and created DILI models using Zebrafish as a model system. The rationale behind selecting these drugs is apart from being the most reported cause of acute liver failure in USA and UK; it is one of the most readily consumed drugs in India too (Larson et al., 2005; Ryder and Beckingham, 2001). Also, in India, where TB is a major health issue, anti-TB drug treatments are responsible for nearly 5% of the mortality rate (Forget and Menzies, 2006). In addition, there are no means to combat these toxicities till now except N-acetylcysteine (NAC) for acetaminophen toxicity (Atkuri et al., 2007; Heard, 2009; Kamalakkannan et al., 2005). Finding the small molecule therapeutics towards this is also attractive and we have tried to address this need too in our study.

1.4 ACETAMINOPHEN (APAP) MEDIATED HEPATOTOXICITY

Acetaminophen is an anti-pyretic and anti-analgesic medication. In overdose conditions, APAP causes complete shutdown of liver function. (William M, 2003). As

APAP enters the liver, it undergoes glucoronidation and sulphation. However a small percentage is acted upon by CYP450 enzymes forming N-acetyl-P-benzoquinone imine (NAPQI), a reactive intermediate metabolite. Usually, NAPQI binds to glutathione (GSH) and the complex is actively expelled out of the cell via biliary secretion. However, in an overdose condition, more NAPQI is synthesized saturating the available GSH and causing its depletion. Further, the NAPQI-GSH complex conjugates with other proteins, nucleic acids and cause MPT. Also, it may cause ROS generation and lipid peroxidation, thus increasing the cell stress and death. Currently, the only treatment available for acetaminophen toxicity is N-acetylcysteine (NAC) (Atkuri et al., 2007; Heard, 2009; Kamalakkannan et al., 2005) and there is an urgent need to come up with more antidotes towards this.

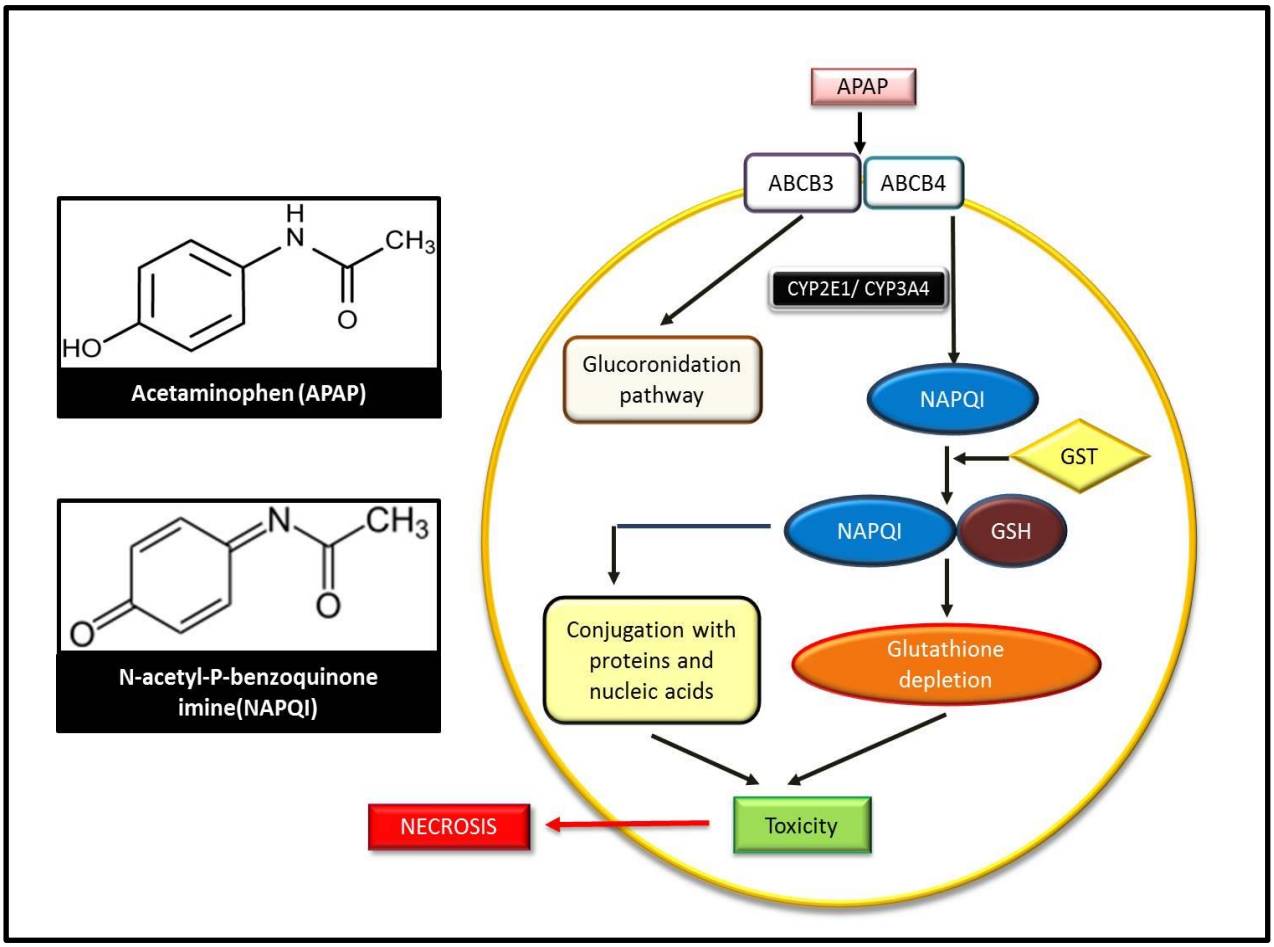

Figure 4: *Acetaminophen hepatotoxicity. APAP enters the cell via ABC family of transporters. CYP enzymes metabolize APAP to N-acetyl-p-benzoquinone imine (NAPQI). Most of the NAPQI is converted to a nontoxic conjugate of NAPQI-GSH (3-Glutathione-S-yl-acetaminophen) by reduction. This reaction is catalysed by glutathione transferase (GST). Recycled NAPQI-GSH adduct causes mitochondrial membrane permeability transition by binding to lysine residues of mitochondrial proteins Lu et al., 2011.*

1.5 ISONIAZID (INH) MEDIATED HEPATOTOXICITY

Isoniazid, when inside the cell, causes formation of intermediate metabolites like Hydrazine and Acetyl hydrazine, the reaction catalysed by NAT2. NAT2 also catalyses the conversion of the acetyl hydrazine to a non-toxic compound, diacetyl hydrazine. Diacetyl hydrazine is easily expelled from the cells. However, in scenarios where these metabolites are acted upon by CYP450 enzymes like CYP2E1, they form toxic metabolites. Accumulation of these within the cell can lead to MPT, oxidative stress, DNA damage and lipid peroxidation. Based on the severity, it can induce cell death (Hassan et al., 2015). No therapies are currently present to counter INH toxicity.

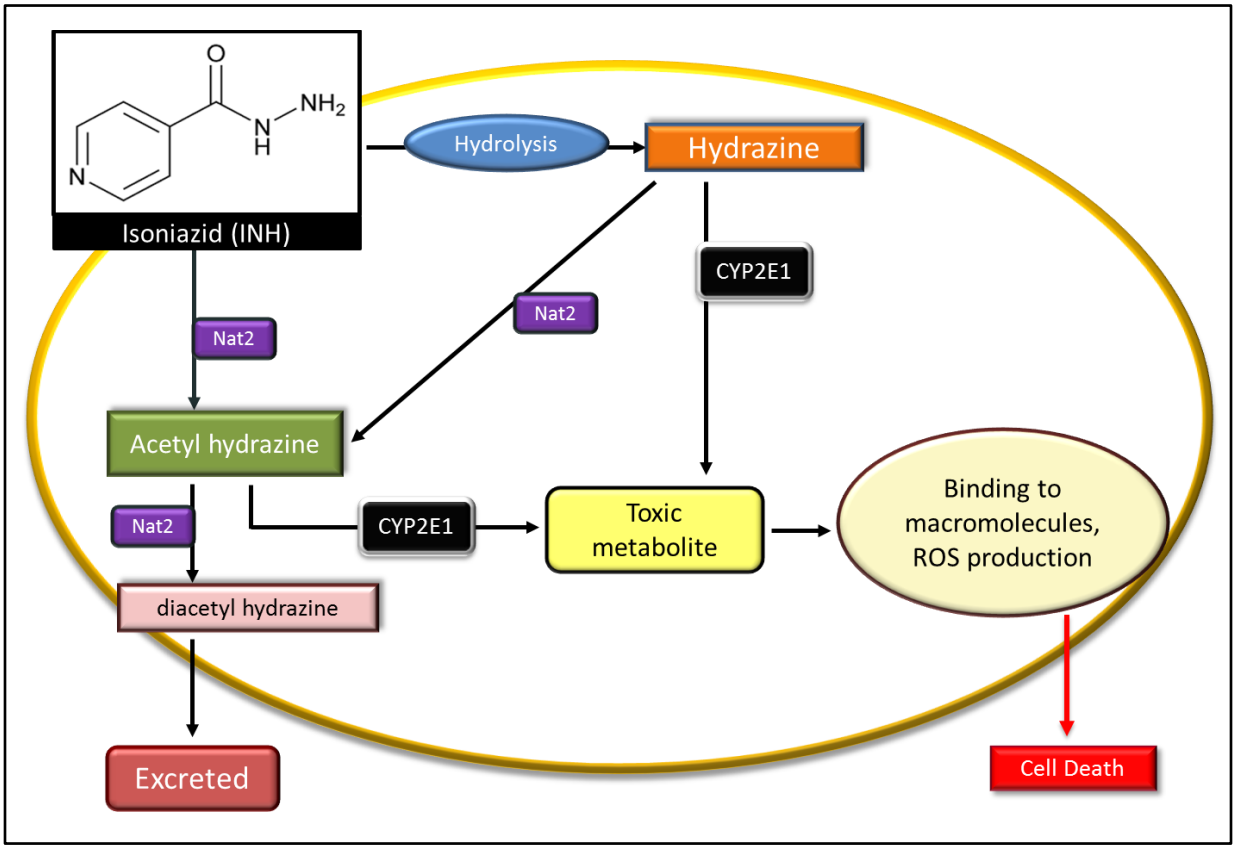

Figure 5: *Isoniazid hepatotoxicity – INH enters the cell and is acted upon by NAT2 which converts it into hydrazine and acetyl hydrazine. NAT2 also converts these metabolites to Diacetyl hydrazine which is excreted from the cell. CYP450 enzymes mainly CYP2E1 convert these metabolites to toxic compounds which cause cell stress and finally cell death (Hassan et al., 2015).*

1.6 ZEBRAFISH AS A MODEL SYSTEM FOR HEPATOTOXICITY

The commonly used models to study hepatotoxicity are rats and mice. Though these serve as wonderful models to study the biology of liver, for the purpose of screening

molecules as therapeutics, these models have certain limitations. As their developmental period is long the studies could be very time consuming. They are difficult to manipulate embryonically and expensive to maintain. They are also not suitable for large scale genetic studies. For such purposes, the model *Danio rerio*, commonly called as Zebrafish has recently evolved to be a popular vertebrate model. It provides many advantages that are suitable for screening drugs. Few of them are listed below –

1. Rapid growth (3-4 days)
2. External fertilization and development
3. High fecundity.
4. Embryos are transparent which makes them easy to manipulate and detect morphological alterations
5. Genetics and developmental biology has been well documented
6. Sequenced genome
7. Many molecular techniques have been developed to study gene functions
8. Easy to create transgenic and mutant fish lines
9. Low maintenance cost and space requirement

With these features, zebrafish has offered a convenient platform for pharmacological, toxicology and molecular screening studies and quickly turned into a favourable model.

1.7 ZEBRAFISH LIVER AND DILI

The liver comprises of various cell types including cholangiocytes, stellate cells, oval cells, endothelial cells and the major population comprising of the parenchymal cells called hepatocytes. Though zebrafish shares all the cell types with humans, however in terms of architecture there are differences (Fig.6) The cellular arrangement is more organized in humans where in Zebrafish it is random. In spite of the structural differences, zebrafish liver is very well conserved to humans in most of the functional aspects. One of the most important functions of liver is the drug metabolism and detoxification where CYP450 enzymes are majorly involved. In Zebrafish, these enzymes were initially characterised by Goldstone and colleagues (2010) wherein they identified 94 CYP genes. Most of the CYP gene families in humans have a single ortholog in zebrafish. However, some CYP families which are involved in exogenous metabolism are more diverse in zebrafish than in humans. Multiple

studies have established that drug metabolism in zebrafish is similar to that of humans (Vliegenthart et al., 2014). For example, in APAP toxicity in humans, CYP3A4 is predominantly required for phase 1 metabolism. Ortholog of CYP3A4 in CYP3A65 in zebrafish was also found to perform the same function (Vliegenthart et al., 2014). Many of such enzymes involved in metabolism of multiple endogenous and exogenous substances in humans are found to be well conserved at the functional level in zebrafish. Hepatotoxicity often leads to inflammatory responses such as immune cell infiltration, cytokine and chemokine secretion etc. The immune responses in DILI are also similar between humans and zebrafish (Vliegenthart et al., 2014).

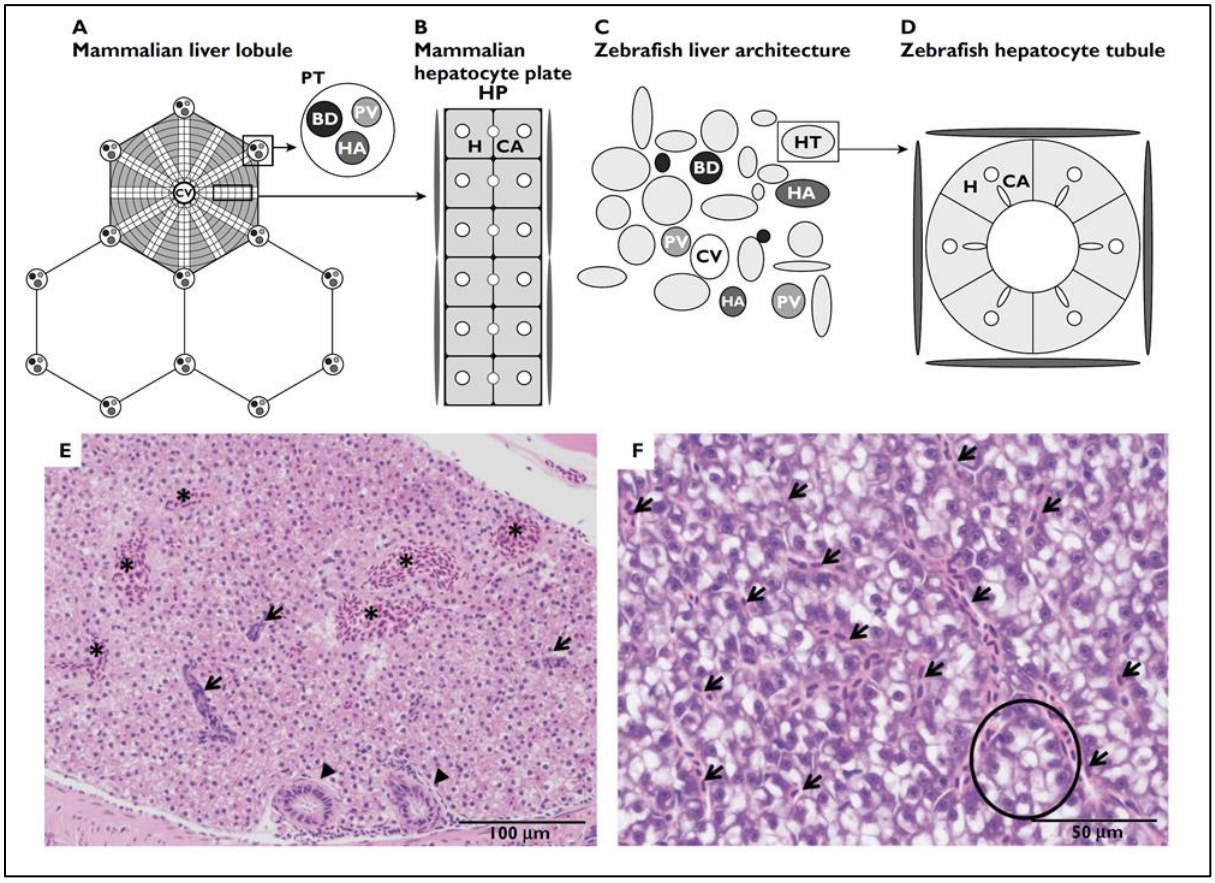

Figure 6: *Graphical representations of mammalian and zebrafish liver architecture demonstrating the differences (transverse section).* ***A)*** *The mammalian architecture depicting hepatocytes aligned as plates emanating outward from the CV. At the sides of every lobule is the PT. The PT contains PV, HA and BD.* ***B)*** *schematic of the mammalian bi-layered hepatocyte plate with CA adjacent to the hepatocyte. However,* ***C)*** *the zebrafish liver architecture is more disorganized when compared to the human liver anatomy. The PV, HA, BD, CV and HT are dispersed all through the parenchyma.* ***D)*** *Depiction of the zebrafish hepatocyte tubule. The hepatocytes and CA are arranged*

around the bile ducts. ***E)*** *and* ***F)*** *H&E staining of male and female zebrafish liver respectively. In* ***E)*** *asterisk depicts blood vessels, arrows, biliary ducts and arrowheads depict bile ductules. In* ***F)*** *the arrows depict sinusoidal spaces and encircled part shows the tubular arrangement of hepatocytes. The figure is taken from Vliegenthart et al., 2014.* [#] ***H: Hepatocytes, HP: Hepatocyte plate, CV: Central Vein, PT: Portal tracts, PV: Portal vein, HA: Hepatic artery, BD: Bile duct, CA: hepatocyte canaliculi, HT: Hepatocyte tubule.***

---

2. MATERIALS AND METHODS

2.1 ZEBRAFISH LINES

- Tu/TuAB fish were used interchangeably and will now be referred as Wild Type (WT).
- Tg(*fabp10a:Gal4-VP16, my17:cerulean*):
  is a double transgenic line, with 1) GFP under *cmlc2* (heart specific) promoter, causing heart to fluoresce green; and 2) Gal4 cloned under *fabp10a* promoter (hepatocyte specific) with Nitroreductasev(NTR)-mCherry fusion protein under UAS. Promoter activity of *fabp10a* via the Gal4-UAS system, leads to synthesis of NTR-mCherry fusion protein causing red fluorescence in liver.

2.2 BREEDING SET UP AND EMBRYO COLLECTION

Male and female fishes were kept in breeding tanks separated by dividers in a maintained temperature zone of 28°C in the dark, overnight. The divider was removed next day, the fishes allowed to mate and embryos were collected. Approximately 100 embryos per 90mm petriplate were sorted and kept at 28°C. 0.003% PTU was added at 1 days post fertilization (dpf) to avoid melanin pigmentation.

2.3 CHEMICAL TREATMENT

2.3.1 CHEMICALS

- Acetaminophen (Sigma A7085) (stock – 2.75M, final concentrations – 15mM and 17.5mM)
- Isoniazid (Sigma I3377) (stock – 1M, final concentrations – 7.5mM and 10mM)
- CSLR001[#] (Stock 10mM, Final concentrations – 1.25µM and 2.5µM)

[#] The name of the molecule coded at CSIR-IGIB

2.3.2 PROTOCOL

All chemical treatments were given at 3dpf in 12/24 well plates with 2/1ml final drug concentration solution respectively. Atmost 25 embryos per well were kept. The stock and required concentrations for each chemical used are given above. All chemical treatments were for 24hrs, at 28°C, post which the embryos were washed with PTU and fixed in 4% PFA for further experiments.

2.4 RIBOPROBE PREPARATION

2.4.1 REAGENTS

Luria Bertani Broth, Ampicillin (Amp), 0.1M Calcium chloride, 15% Glycerol, Nuclease free water, Restriction Digestion enzymes (Sal1 HF, Not I from NEB) Luria Bertani (LB) agar, Phenol:Chlororform:Isoamyl alcohol, Isopropanol, 70% Ethanol, 80% Glycerol, SOC media, QIAprep spin miniprep kit, RNA purification columns, IVT DIG-labelling RNA kit: Roche – 10XBuffer, DIG labeled NTP's, Rnase inhibitor, Enzyme (SP6, T7 RNA polymerase), Nuclease Free Water (NFW)

2.4.2 PROTOCOL

TRANSFORMATION

In 100µl of DH5α competent cells, 5µl of the required plasmid was added followed by incubation on ice for 30mins. Heat Shock was given to cells for 30sec at 42ºC followed by ice incubation for 20mins. 250µl of SOC media was added and solution was kept on shaker at 37ºC for 1hr. Each of the transformed samples was spread on LB Amp+ agar plates and incubated overnight at 37ºC.

PREPARATION FOR PLASMID ISOLATION

To about 5ml of LB Broth, 1 colony was added using T-200 tips. Sealed falcon was kept on shaker incubator overnight. The falcon was centrifuged at 4000rpm for 5mins. Supernatant was decanted and the pellet was kept in -20ºC.

PLASMID DNA PURIFICATION USING THE QIAPREP SPIN MINIPREP KIT

The bacterial pellets were resuspended in 250µl of buffer P1 and transferred to a microcentrifuge tube. 250µl of buffer P2 was added and mixed thoroughly by inverting the tube 4-6 times. 350µl of Buffer N3 was added and solution was mixed immediately and thoroughly by inverting the tube 4-6 times. The tubes were

centrifuged for 10min at 13000 rpm in a tabletop microcentrifuge. The supernatant was added to the QIAprep spin column by decanting or by pipetting and was then centrifuged for 30-60secs. The flow through was discarded. The QIAprep spin column was washed by adding 0.5ml of Buffer PB and then centrifuged for 30-60 sec. Again the flow through was discarded. The QIAprep spin column was washed by adding 0.75 ml buffer PE and was centrifuged for 30-60 sec. The flow through was discarded and columns were centrifuged at full speed for 1min to remove residual additional wash buffer. QIAprep column was placed in a clean 1.5ml microcentrifuge tube. DNA was eluted by adding 50µl of Buffer EB or water to the center of the QIAprep spin column and allowed to stand for 1min and then centrifuged for 1min.

RESTRICTION DIGESTION

In each eppendorf, 2.5µl of 10XBuffer, 0.25µl of BSA, 2µg of the required plasmid, 2 Unit of the required digestion enzyme was added. NF water was added to get the final volume as 25µl. The eppendorfs were kept in -20ºC overnight.

PLASMID PURIFICATION

To the digested plasmid equal amount of phenol:chloroform:Iso-amylalcohol was added. The eppendorfs were spun at 13000rpm for 5mins at 4°C. Supernatant were transferred in a fresh eppendorf and 0.7 times the volume of isopropanol was added. The solution was mixed by tapping followed by a spin down at 13000rpm for 10mins at RT. The pellet is retained and supernatant discarded. 500µl of 70% ethanol was added followed by a spin at 13000rpm for 5min at RT. Ethanol was removed and the pellet air dried for about 20mins and resuspended in 20µl NFW.

IN VITRO TRANSCRIPTION

To 1µg of the required plasmid, 2µl of 10XBuffer, 2µl of DIG labeled NTP's, 2µl of the required RNA polymerase and 1µl of *Rnase* inhibitor was added. Required quantity of NFW was added to make the volume up to 20µl.The eppendorfs were kept at 37ºC for 4hrs and later stored in -20ºC.

PURIFICATION

RNA purification columns were used. These columns were kept in eppendorfs and spun for 1min at 1000rcf to remove the buffer. Post IVT RNA is added to the columns (in fresh eppendorfs) and spun at 1000rcf for 4min. The eppendorfs now

contains purified RNA probes. Based on the concentration, they are mixed in an appropriate volume of Hybridization mix (given below).

2.5 IN-SITU HYBRIDIZATION

2.5.1 REAGENTS

4% PFA, PBS+0.01%Tween (PTw), Methanol, Proteinase K (Roche 03115879001), Hybridization wash, Hybridization mix, AP-anti-DIG antibody (Roche 11093274910), Fetal bovine serum (FBS), Tris-buffered saline and Tween-20 (TBST), NTMT, Nitro blue tetrazolium (NBT) 100mg/mL and 5-bromo-4-chloro-3-indolyl-phosphate (BCIP) 50 mg/mL.

Hybridization mix

REAGENTS	***FINAL CONC.***	***VOLUME***
Formaldehyde (Fluka 47670)	50%	25 ml
SSC (20x pH5 w citric acid!!)	1.3xSSC	3.25ml
EDTA (0.5M, pH8)	5 mM	0.5ml
Yeast RNA (50mg/ml) (Sigma R-7125)	50 µg/ml	50 µl
Tween-20 (10%)	0.2%	100 µl
Heparin (100mg/ml) (sigma H-3400)	100 µg/ml	50 µl
Water		To volume
	Total volume	50ml

Hybridization wash: All the reagents remained same as Hybridization mix except yeast RNA and heparin are not added

10XTBST

REAGENTS	***VOLUME***
5M NaCl	27.4ml
1M KCl	2.7ml
1M Tris-Cl (pH 7.5)	25ml
Tween-20	100 µl
Total	100ml

NTMT

REAGENTS	***FINAL CONC.***	***VOLUME***
5M NaCl	0.1M	1 ml
1M Tris-HCl (pH 9.5)	0.1M	5ml
1M MgCl2	0.05M	0.25ml
Tween-20	1%	0.5ml
Water		To volume
	Total volume	

2.5.2 PROBES

- *fabp10a* riboprobe
- *hamp* riboprobe

2.5.3 PROTOCOL

METHANOL FIXATION EMBRYOS (Day 1)

Embryos fixed in 4% PFA were washed with PTw, twice, followed by a wash with 50% MeOH/PTw and stored in 100% MeOH overnight.

PRETREATMENT AND HYBRIDIZATION (Day 2)

Embryos were rehydrated through 50% MeOH/PTw and washed twice with PTw. Since the embryos were fixed at 4dpf, they were incubated in Proteinase K (1µl in 1ml PTw) for 14mins. This is followed by a PTw wash and incubation in 4% PFA for 20mins. Again, PTw washes were given. This was followed by a wash with 1:1 PTw/Hybridization wash (pre-warmed at 65ºC) and a wash with 1ml Hybridization Wash (pre-warmed at 65ºC). Embryos are allowed to settle. The embryos were incubated in 1ml Hybridization mix (pre-warmed at 65ºC) for >1hr at 65ºC. 1ml of pre-warmed DIG-labelled RNA probe in Hybridization mix was added and placed at 65ºC overnight.

POST HYBRIDIZATION (Day 3)

Probe was removed and two washes with Hybridization wash were given at 65ºC for 30min, followed by a rinse with 1XTBST at RT. They were incubated in 1XTBST at RT for 15mins. The embryos were then incubated for 1hr with 1XTBST+10% heat inactivated sheep serum (FBS) at RT, followed by an incubation for 4hr with 1XTBST+10% FBS + 1/3000 dilution of AP-anti-DIG-antibody. Post incubation, they were rinsed twice with 1XTBST and left overnight in 1XTBST in 4ºC.

HISTOCHEMISTRY (Day 4)

Embryos were transferred into 12-well plates and washed with 1ml NTMT for 10mins. They were then incubated with NBT/BCIP (50µl NBT and 37.5µl BCIP in 10ml NTMT) and monitored for colour reaction. Upon colour development, the reaction was stopped by giving PTw washes and then storing embryos in 4% Paraformaldehyde.

2.6 WESTERN BLOT

2.6.1 REAGENTS

NP40 Lysis buffer, BCA kit (Invitrogen®), Bovine Serum Albumin (BSA) (1mg/ml), Resolving and Stacking Gel (given below), Protein loading dye, 5% BSA, 3-color prestained protein ladder (Puregene, PG-PMT 2922)1° rabbit anti-mCherry antibody (Abcam ab167453, 1:5000 dilution in 2% BSA), 1° rabbit anti-β-actin antibody (Cell Signalling 46972, 1:5000 dilution in 2% BSA), 2° anti-rabbit IgG, HRP-linked antibody (Cell Signalling, 7074P2, 1:10000 in 2% BSA), Immobilon western (chemiluminescent HRP substrate, Millipore – WBKLS0500)

SDS-PAGE Gels:

Materials	***Resolving gel (12%)***	***Stacking gel (5%)***
Water	3.3 mL	3.2 mL
30% Acrylamide	4.0 mL	0.83 mL
1.5M Tris(Ph8.8)	2.5 mL	0.63 mL
10% SDS	0.1 mL	0.05 mL
10% Ammonium per sulphate	0.1 mL	0.05 mL
TEMED	0.004 mL	0.005 mL
Total Volume	10ml	5ml

2.6.2 PROTOCOL

PROTEIN ISOLATION

Approximately 25 embryos per sample were lysed using 50µL of NP40 lysis buffer. The samples were spun at 10000 rpm for 15min and supernatant containing proteins was collected in a fresh eppendorf.

BIO CHRONIC ASSAY

With the help of BCA kit (Invitrogen®), sequential concentrations of BSA were tested and a standard graph was generated using TECAN. The equation so obtained from the linear trendline was used to obtain the concentration of the required sample (Every sample was tested in duplicates.)

SDS PAGE

Protein samples were mixed with a denaturing dye containing sodium dodecyl sulphate and heated at 95º C for 10mins. Samples were spun down and loaded onto SDS-PAGE gel and allowed to resolve completely at 120V.

TRANSFER

After gel resolution, proteins were transferred to a PVDF membrane, pre-activated by methanol. The activated membrane was placed next to the gel and a sandwich was made with a layer of filter papers on both the sides. The sandwich was placed into the transfer machinery and 1X Transfer Buffer was added. Protein transfer was kept for two hours at 70V.

BLOTTING

The membrane was kept in 5% BSA solution for blocking for 2hrs at 4ºC followed by incubation in anti-mCherry primary antibody, overnight at 4ºC. Blot was washed with 1XTBST, thrice, 15mins each, followed by secondary antibody incubation for 1.5hrs at RT. Blot was again washed in 1XTBST, thrice, 15mins each and developed in dark by using Immobilon western chemiluminescent HRP substrate (Millipore) and imaged. The blot was stripped off any antibody using the stripping buffer and process was repeated for β-actin from blocking

2.7 QUANTITATIVE REAL TIME – POLYMERASE CHAIN REACTION (qRT-PCR)

2.7.1 REAGENTS

Trizol (Invitrogen), Chloroform, Isopropanol, 85% Ethanol, Nuclease free water (NFW), QuantiTect reverse transcriptase kit (QIAGEN, 205311), Primers

2.7.2 PROTOCOL

RNA ISOLATION

Embryos were fixed in 200µl Trizol and homogenized using the tissue homogenizer. 800µl Trizol was added followed by 200µl of Chloroform and mixed by inverting. The solution was let to stand for 3mins. The solution was centrifuged at 14000 rpm, 4°C for 15mins and the supernatant transferred to new eppendorf tube. 500µl of chilled

isopropanol was added and mixed by inverting followed by centrifugation at 14000 rpm, 4°C for 10mins. The supernatant was decanted and 85% ethanol was added to the tube and centrifuged at 14000 rpm, 4°C for 5mins, twice. Ethanol was removed and pellet was dried at 65°C for 10mins. Pellet was resuspended in 20µl NFW and stored at -20°C. 1µl RNA sample was loaded in 1.5 % agarose gel to check the quality of the product.

cDNA PREPARATION

RNA was thawed at 65°C for 5mins. To 1µg of RNA, 2µl of gDNA wipe-out buffer was added. NFW was added to make the volume to 14µl**.** The solution was incubated at 42°C for 2mins in the thermo cycler and 6µl of the transcription master mix (given below) was added and incubated for 15 min at 42°C followed by 3 min at 95°C to stop the reverse transcriptase action. Finally, cDNA was stored at -20°C.

Transcription Master Mix - 4µl RT Buffer, 1µl Primer mix, 1µl reverse transcriptase enzyme.

QUANTITATIVE REAL TIME PCR

cDNA were used for qRT-PCR. Two sets of master mix were prepared as following.

Reagents	***Volume (µl)***
MASTER MIX 1	
Fast Start Essential DNA Green master (Sybr Green) Roche 06 924 204 001	10µl
Forward primer (1:10 diluted in NFW)	1µl
Reverse primer (1:10 diluted in NFW)	1µl
MASTER MIX 2	
cDNA (1:3 diluted in NFW)	1µl
NFW	7µl
Total	20µl

These two master mixes were added in qRT-PCR plates to make the volume upto 20µl reaction/well.

2.8 DCFDA ASSAY

2.8.1 REAGENT

H_2O_2, 2',7'–dichlorofluorescin diacetate (DCFDA), 0.003%PTU, INFINITE M200 PRO from TECAN was used to measure the fluorescence.

2.8.2 Protocol

Master solution of 0.005 v/v% of DCFDA was made in 0.003% PTU. In a 96-well transparent flat bottom plate, 3 embryos/well (5 wells per treatment) were added and excess solution drained. 200µl of the Master solution was added to each well. Apart from the treatments, 1 set of wells only contained the master solution ("Blank"). Another set of wells contained untreated embryos to which 0.00005 v/v% of H_2O_2 in the master solution was added. Next, the plate was incubated in 37°C for 30mins and INFINITE M200 PRO was used to take fluorescent reading at regular intervals of 15mins. Total number of cycles was 25.

2.9 HEMATOXYLIN AND EOSIN (H&E) STAINING

2.9.1 REAGENT

Xylene (Sigma), Hematoxylin (Himedia), Eosin (Himedia), Ethanol, 0.08% Ammonium solution

2.9.2 METHOD

For H&E staining, sections were incubated in Xylene for 10mins followed by washes in decreasing gradient of ethanol (in the order - 100%, 70% and 50% ethanol). They were stained with Mayer's Hematoxylin and washed in water. 0.08% of Ammonium solution was added for 30secs and sections washed in water. The sections were counterstained with Eosin (in water) and Eosin (in ethanol) for 1 min each. Sections were washed in gradually increasing concentration of ethanol (in the respective order 50%, 70% and 100% and incubated in Xylene for 10mins. Mounting was done using DPX mount media and coverslips.

2.10 MICROSCOPY AND SECTIONING

Isolated liver were sectioned using cryotome Leica CM 1850.

Imaging of fluorescent transgenic embryos were done using – Zeiss Axioscope A1
Imaging of In-situ hybridized embryos were done using – Zeiss Stemi 200C
Imaging of liver tissues samples were done using – Nikon Eclipse T*i*-U

2.11 QUANTIFICATION AND ANALYSIS

ImageJ software was used for quantification of ISH analysis, fluorescent analysis and western blot analysis.

GraphPad Prism Version 5.0 was used to prepare all the graphs

2.12 STATISTICAL ANALYSIS

Student *t*-test, two tailed for unequal variance (Welch's *t*-test) was used for all quantifications.

P value Wording Summary -

< 0.0001 - Very significant (********)

< 0.001 - Very significant (*******)

0.001 to 0.01 - Very significant (******)

0.01 to 0.05 - Significant (*****)

≥ 0.05 - Not significant (n.s.)

3. RESULTS

3.1 HEPATOTOXICITY BY ACETAMINOPHEN (APAP) AND ISONIAZID (INH) TREATMENT

3.1.1 Hepatotoxicity due to acetaminophen (APAP)

To assess APAP toxicity, WT embryos were treated at 3 days post fertilization (dpf) for 24hrs with various concentrations of Acetaminophen, and their survival was noted. Concentrations beyond 20mM APAP for 24hrs were fatal to the embryos as suggested by the decrease in the survival rate (Fig 7B). The treatment concentrations were selected based on the literature available(North et al., 2010; Weigt et al., 2010). We fixed the APAP-treated embryos with 4% PFA and performed RNA in-situ hybridization (RNA-ISH) using the *fabp10a* riboprobe as per the protocol given in materials and methods. *fabp10a* expression is shown to be limited to the hepatocytes in the liver and therefore can be used as a marker for liver size (North et al., 2010; Zhang et al., 2014). We found significant down-regulation in the *fabp10a* transcript level by RNA-ISH for concentrations above 15mM (Fig 7C). As the survival was highly compromised with 20mM APAP (Fig 7B), concentrations above 20mM were not suitable. Based on the survival and extent of liver damage by *fabp10a* riboprobe expression, we selected 15mM and 17.5mM concentrations of APAP for further studies. Both concentrations caused significant liver damage without any effect on the survival. Decreased expression of *fabp10a* observed in

RNA-ISH was also supported by qRT-PCR (Fig 7D). In order to test the effect of APAP on a completely developed liver, we treated adult zebrafish with various concentration of APAP. APAP 7.5mM concentration for 24hrs was standardized post which the fish was dissected and liver isolated. Upon dissection a visible colour difference was observed between the control and APAP treated samples (Fig 7F). H&E stained section showed a significantly distorted architecture in APAP treated samples (Fig 7G). Increased intercellular spaces suggest tissue damage (Fig 7G).

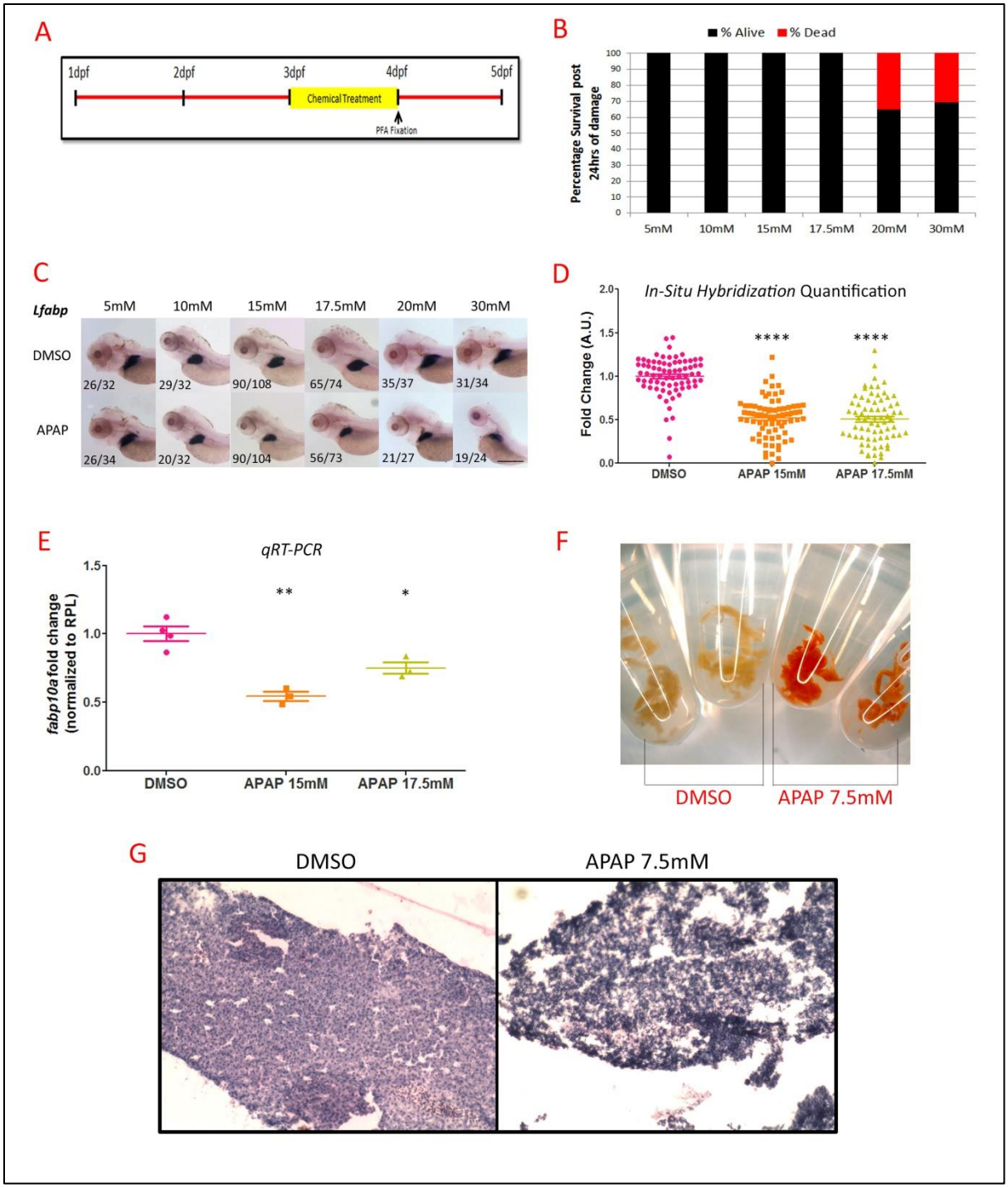

Figure 7: *Hepatotoxicity with APAP.* ***A)*** *Experimental timeline for damage treatment. Embryos were treated with APAP at 3dpf for 24hrs and fixed in 4% PFA for further experiments.* ***B)*** *Survival graph for concentration standardization of APAP. Note the decrease in survival post 20mM concentration.* ***C)*** *In-situ Hybridization using fabp10a riboprobe for different concentrations of APAP. Scale bar – 0.5mm. Based on this data and survival chart, concentrations 15 and 17.5mM APAP were decided upon.* ***D)*** *Quantification of ISH using ImageJ software. Y-axis: Fold change of fabp10a, arbitrary units (A.U.). Both the concentration show significant downregulation.* ***E)*** *qRT-PCR estimation of fabp10a. Y-axis: Fold change of fabp10a transcript normalized to RPL. Again both concentrations of APAP show*

significant downregulation. ***F)*** *Adult zebrafish were treated for 24hrs with 7.5mM APAP and liver were isolated upon dissection. Note the difference in colour between DMSO and APAP treated samples.* ***G)*** *H&E staining of isolated liver from adult zebrafish. Note the presence of increased intercellular spaces in APAP treated liver which indicate damage. Magnification – 10X.*

3.1.2 Hepatotoxicity due to Isoniazid (INH)

To assess the hepatotoxicity caused by INH, WT embryos were treated at 3dpf with different concentrations of INH and the survival was noted with increasing time. High death was observed in concentration 100 and 50mM by 18hrs and 22hrs post damage respectively. No decrease in survival was observed for concentrations 2.5mM, 5mM, 10mM and 20mM till 24hrs post which the lethality increased (Fig 8A). Based on this data, (Fig 8A) we limited INH treatment time for 24hrs (Fig 8B) and using various concentrations i.e. from 5mM to 20mM, we performed RNA-ISH using the *fabp10a* riboprobe. *Fabp10a* expression showed significant down-regulation for all the concentrations beyond 7.5mM indicating liver damage in these embryos. However, embryos treated with higher concentrations i.e. 15mM and 20mM showed affected survival even after the INH treatment was removed. 20mM INH also caused multiple morphological defects during the treatment time itself (Image not shown). We therefore limited INH concentration to INH 7.5mM and INH 10mM for the period of 24 hours. As mentioned earlier, both concentrations showed significant down-regulation in *fabp10a* expression by RNA-ISH (Fig 8C and Fig 8D). It was also supported by qRT-PCR (Fig2E). Most importantly, the embryos were able to survive after the INH treatment was removed. We further performed the INH treatment to adult Zebrafish. 24hours of INH exposure (2mM) was found to be sufficient to cause significant damage to liver. As shown in Fig.2F, INH treated adult liver sections show completely distorted architecture. Large intracellular spaces were observed with huge focal haemorrhage indicating that INH, a medically prescribed drug, can be a potent hepatotoxin if taken at high dose.

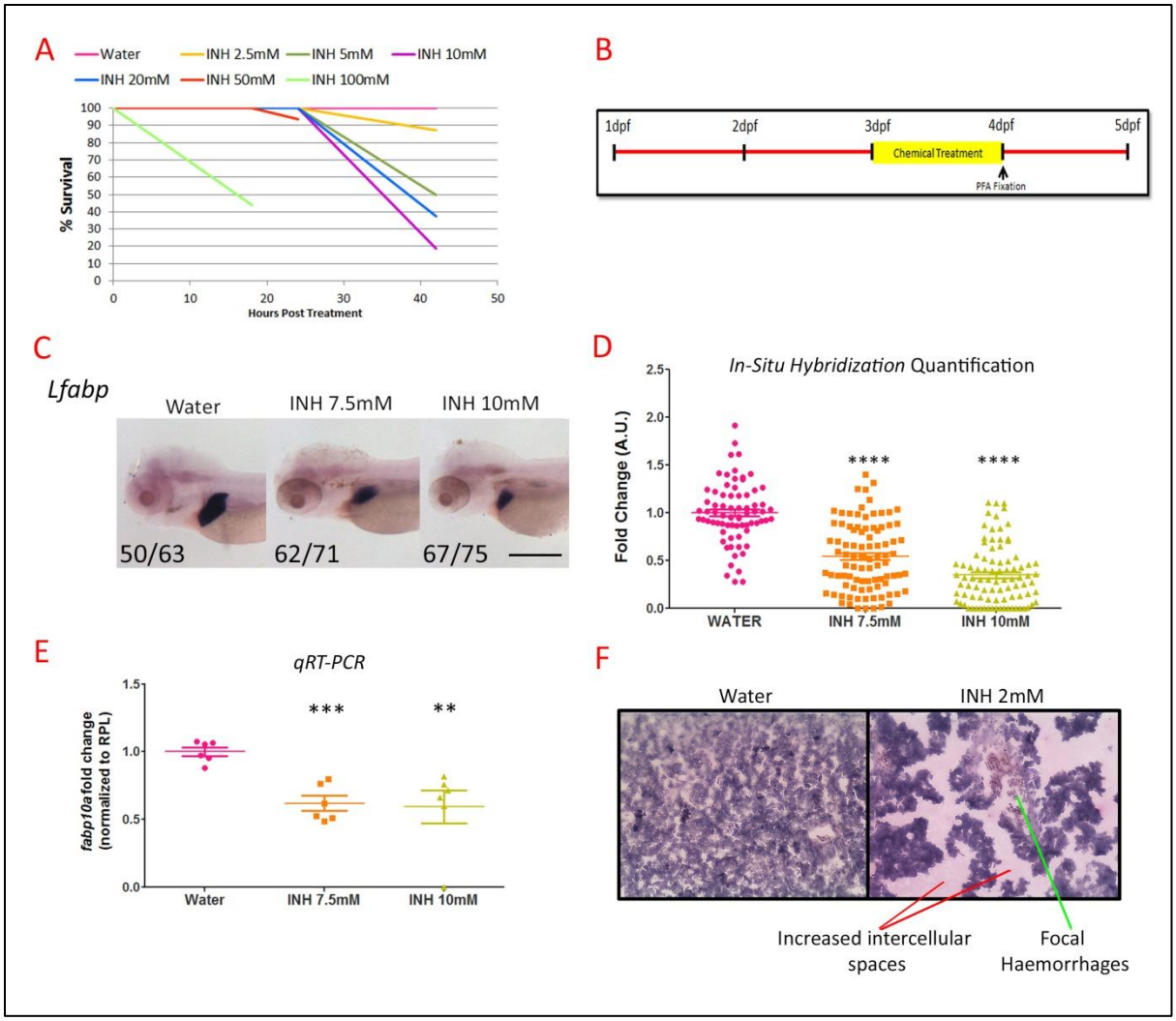

Figure 8: *Hepatotoxicity with INH.* ***A)*** *Survival graph vs. hours post treatment for concentration standardization of INH.* ***B)*** *Experimental timeline for damage treatment. Embryos were treated with INH at 3dpf for 24hrs and fixed in 4% PFA for further experiments.* ***C)*** *In-situ Hybridization using fabp10a riboprobe for 7.5mM and 10mM INH. Scale Bar – 0.5mm.* ***D)*** *Quantification of ISH using ImageJ software. Both the concentration show significant downregulation.* ***E)*** *qRT-PCR estimation of fabp10a. Again both concentrations of APAP show significant downregulation. Y-axis: Fold change of fabp10a normalized to RPL.* ***F)*** *Adult zebrafish were treated for 24hrs with 2mM INH and liver were isolated upon dissection. H&E staining of isolated liver sections indicates increased intercellular spaces and increased haemorrhages in INH treated liver which indicates damage. Magnification – 20X.*

3.1.3 Assessment of hepatotoxicity due to APAP and INH using transgenic line Tg(fabp10a:Gal4-VP16, my17:cerulean)

As given in materials and methods, we have a double transgenic line, Tg(*fabp10a:Gal4-VP16, my17:cerulean*) with green heart (GFP) and red liver (mCherry) thereby giving us an advantage of visualising these organs in live embryos. To support the hepatotoxicity caused by APAP and INH, we took advantage of this line (Fig 9A). This transgenic also offers genetic way of specifically ablating hepatocytes. The transgenic systemically expresses Nitroreductase (NTR), a bacterial enzyme. NTR is fused to mCherry and its expression is dependent on UAS activation. Gal4 is under the *fabp10a* promoter. When a drug, Metronidazole (MTZ) is added, it is reduced by NTR forming a toxic by-product therefore causing cell death. Since, *fabp10a* is expressed in hepatocytes; MTZ treatment causes hepatocyte specific ablation and mCherry fluorescence can be used as the readout. Using this line, we tested the drugs APAP and INH using the standardized protocol. The mCherry fluorescence from liver was captured using fluorescence microscope (Fig 9B) and images were quantified using ImageJ software. In support of our RNA-ISH and qRT-PCR, mCherry fluorescence also showed reduction upon APAP and INH treatment. There was however high variability observed as can be seen in the Fig. 9C. This can be attributed to the level of integration of the construct. To rule out that the reduction in liver size is not a mere loss of fluorescence, we checked the mCherry protein levels by western blot. β-actin served as the loading control. We found significant decrease in mCherry protein (normalized to β-actin) for both the drugs. Fig 9D represents quantification of multiple experiments.

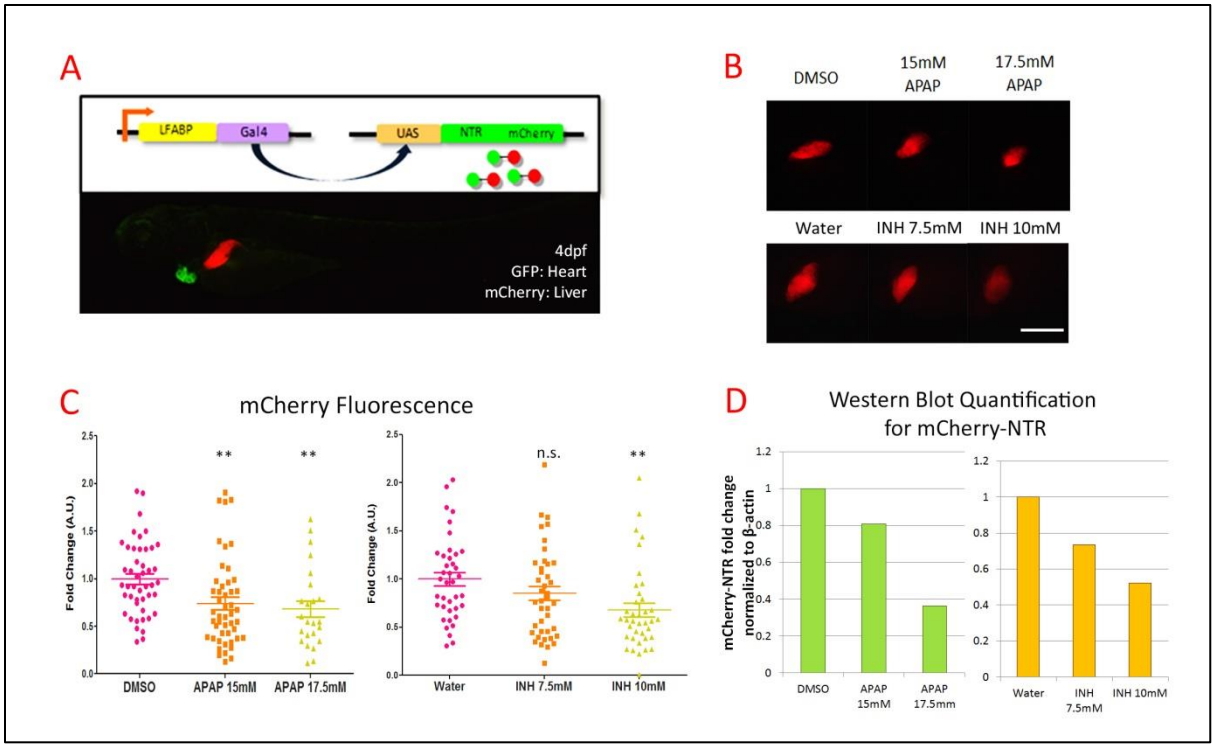

Figure 9: *Assessment of hepatotoxicity due to APAP and INH using transgenic line Tg(fabp10a:Gal4-VP16, my17:cerulean).* ***A)*** *figure shows the Tg(fabp10a:Gal4-VP16, my17:cerulean) transgenic line with green heart and red liver.* ***B)*** *Transgenic embryos were treated with APAP/INH at 3dpf for 24hrs and fixed in 4% PFA for Imaging. Both the drug concentrations show some decrease in mCherry fluorescence. Scale bar: 0.25mm. This is more evident in* ***C)*** *quantification of fluorescent images using ImageJ software. Both the concentrations of INH/APAP show significant downregulation. Y-axis: Fold change (A.U.).* ***D)*** *To validate the results, we performed western blot for mCherry.* β*-actin was used the loading control. The representative graph of western blot analysis is given above. Fold change of mCherry (normalized to* β*-actin) shows decrease for all concentrations for both INH as well as APAP.*

3.2 CHARACTERIZATION OF HEPATOTOXICITY POST TREATMENT WITH ACETAMINOPHEN AND INH

3.2.1 Estimation of ROS

Reactive Oxygen species (ROS) is one of the well-known causes of cell toxicity. In order to check if this is the cause behind APAP and INH toxicity, we performed DCFDA assay. 2',7'–dichlorofluorescin diacetate (DCFDA) is non-fluorescent molecule. When it enters the cell, upon encountering ROS the molecule converts to a fluorescent molecule. The extent of fluorescence is directly proportional to the

amount of ROS present within the cell. The fluorescence value can be measured by using fluorescent detectors (infinite M200 PRO from TECAN). All the tested concentrations of APAP and INH showed higher ROS levels when compared to their respective controls (Fig 10). This suggests that both APAP and INH damage induce oxidative stress in the embryos.

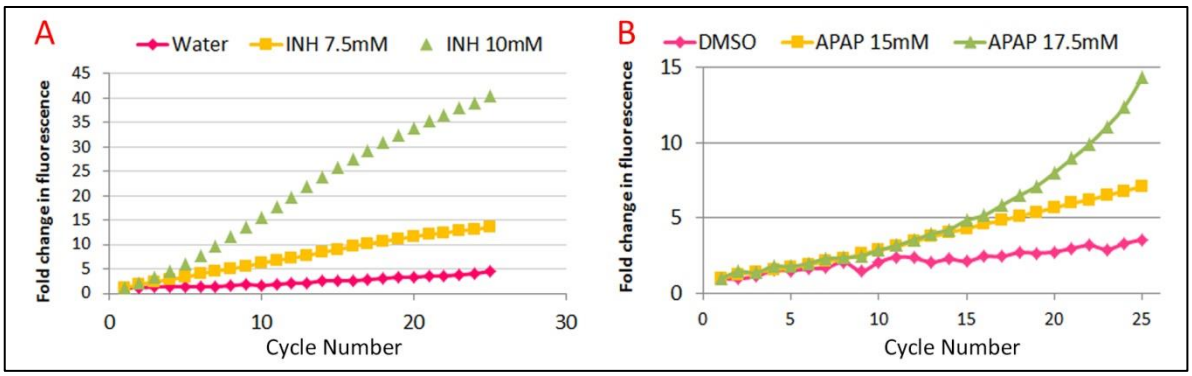

Figure 10: A) *DCFDA Assay for 7.5 and 10mM INH. ROS is upregulated for both when compared to the water control. 10mM is more upregulated than 7.5mM INH.* ***B)*** *DCFDA Assay for 15 and 17.5mM APAP. ROS is upregulated for both when compared to the water control. 17.5mM is more upregulated than 15mM INH. Both drugs show concentration dependent upregulation in ROS levels. Y-axis: Fold change in fluorescence*

3.2.2 Characterization of APAP Damage

After confirming by multiple ways that APAP causes liver damage, we went on to characterise this phenomenon. We checked the status of few other liver specific genes including *HAMP* (Fig 11A and Fig 11B), *Ceruloplasmin* (Fig 11C) and IGFBP1a (Fig 11D) by qRT-PCR. To our surprise, we found an increase in the transcript levels of these genes. The same was also observed in ISH using *HAMP* riboprobe in both the tested concentrations (Fig.11A). For cell death, apoptosis markers like *caspase8* and *BAD* were tested. Preliminary experiments suggest an up-regulation in case of *BAD* when treated with 17.5mM APAP (Fig 11E and Fig 11F). Though not significant, c*aspase8* did show an increasing trend. These experiments are to be repeated to confirm the same. In all, our data suggests that APAP might be causing ROS production and thereby leading to apoptosis and together, liver damage. Confirmatory experiments for this hypothesis however, are needed.

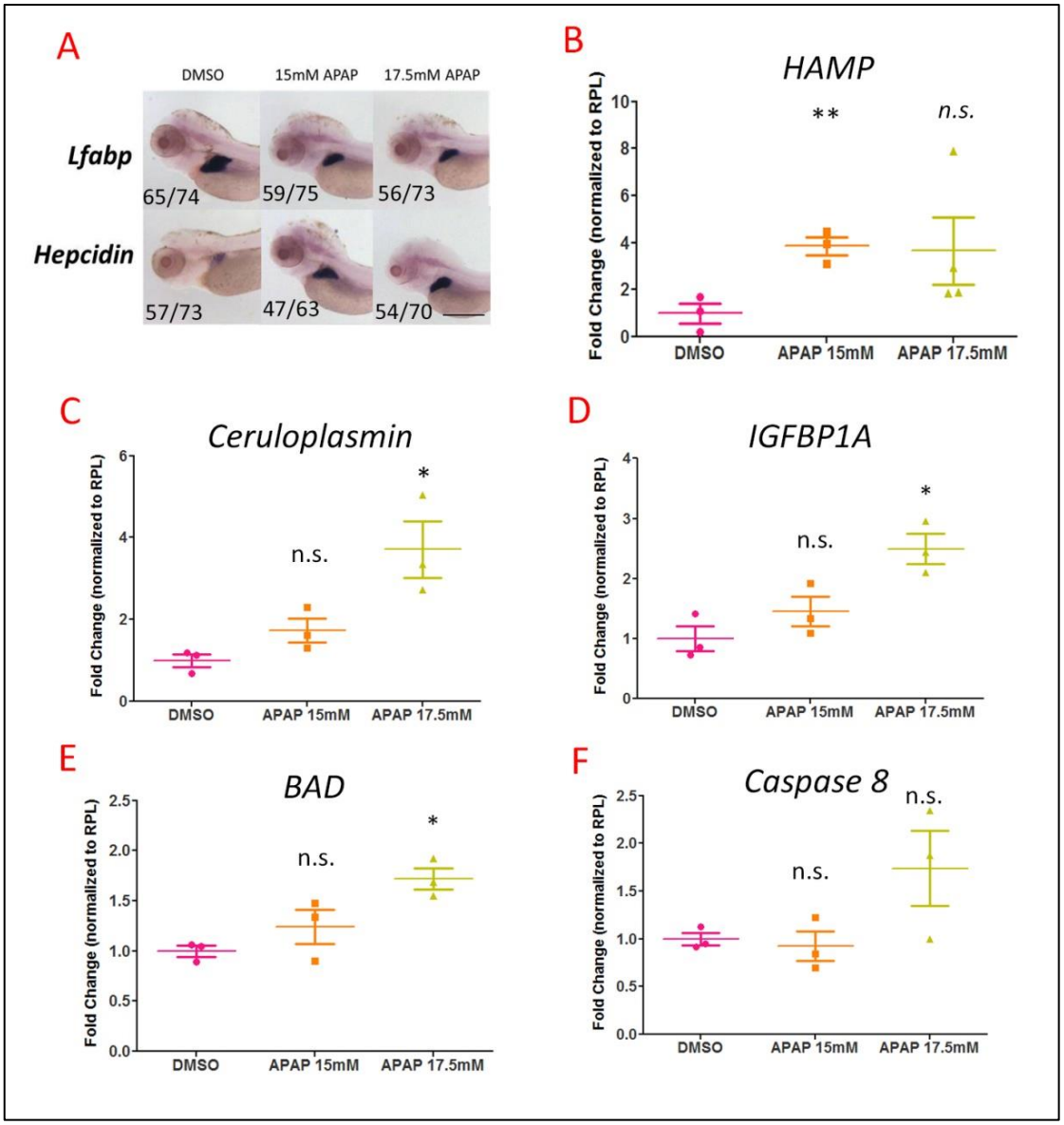

Figure 11: A) *ISH for Hamp shows upregulation in expression for both APAP concentrations. Scale bar: 0.5mm. qRT-PCR for* ***B)*** *HAMP, other liver specific primers like* ***C)*** *Ceruloplasmin and* ***D)*** *IGFBP1A, apoptosis markers like* ***E)*** *BAD* ***and F)*** *Caspase8. Y-axis denotes Fold change of transcript (normalized to RPL). Please note that all qRT-PCR's have to be repeated.*

3.2.3 Characterization of INH Damage

Like APAP, INH treated embryos also showed high upregulation of *HAMP* by RNA-ISH (Fig 12A). This was also checked by qRT–PCR which showed nearly 40 fold induction in HAMP transcript levels (Fig 12B). Apart from *HAMP*, other liver markers like *ceruloplasmin*, *aldob* and *IGFBP1a* levels were also tested for transcript levels and except Aldob, all the genes showed upregulation (Fig 12C and 12D).

Various markers of apoptosis like *caspase8*, *BAX*, *BAD* and Death domain-containing protein *CRADD* were tested (Fig 12E) and most showed significant induction upon INH treatment with nearly both the concentrations tested suggesting apoptosis as a culprit for INH mediated toxicity.

Further we checked the status of other parameters of cell stress including inflammation, ROS, ER and mitochondrial stress etc. We checked Inflammation using level of genes *IL-1β and C3a.1* and found them to increase upon 10mM INH treatment (Fig 12F). For ROS, *nrf2* and *sod* were tested. *Nrf2* showed significant upregulation whereas *sod* did not (Fig 12G). *BIP*, *CHOP* and *PERK* served as the markers of ER stress. Apart from *BIP*, both *CHOP* and *PERK* showed upregulation upon INH treatment (Fig 12H). For Mitochondrial stress, *UCP2* and *COX2* genes were tested. Although *UCP2* is upregulated in INH treatment, *COX2* did not show the same (Fig 12I). *CYP1A1* which is an established marker of detoxification was also found to be upregulated upon INH (10mM) treatment (Fig 12J). Our results suggest that INH mediated liver damage involves many of the parameters of cell toxicity i.e. inflammation, ER and mitochondrial stress. However, more studies to support the same are needed.

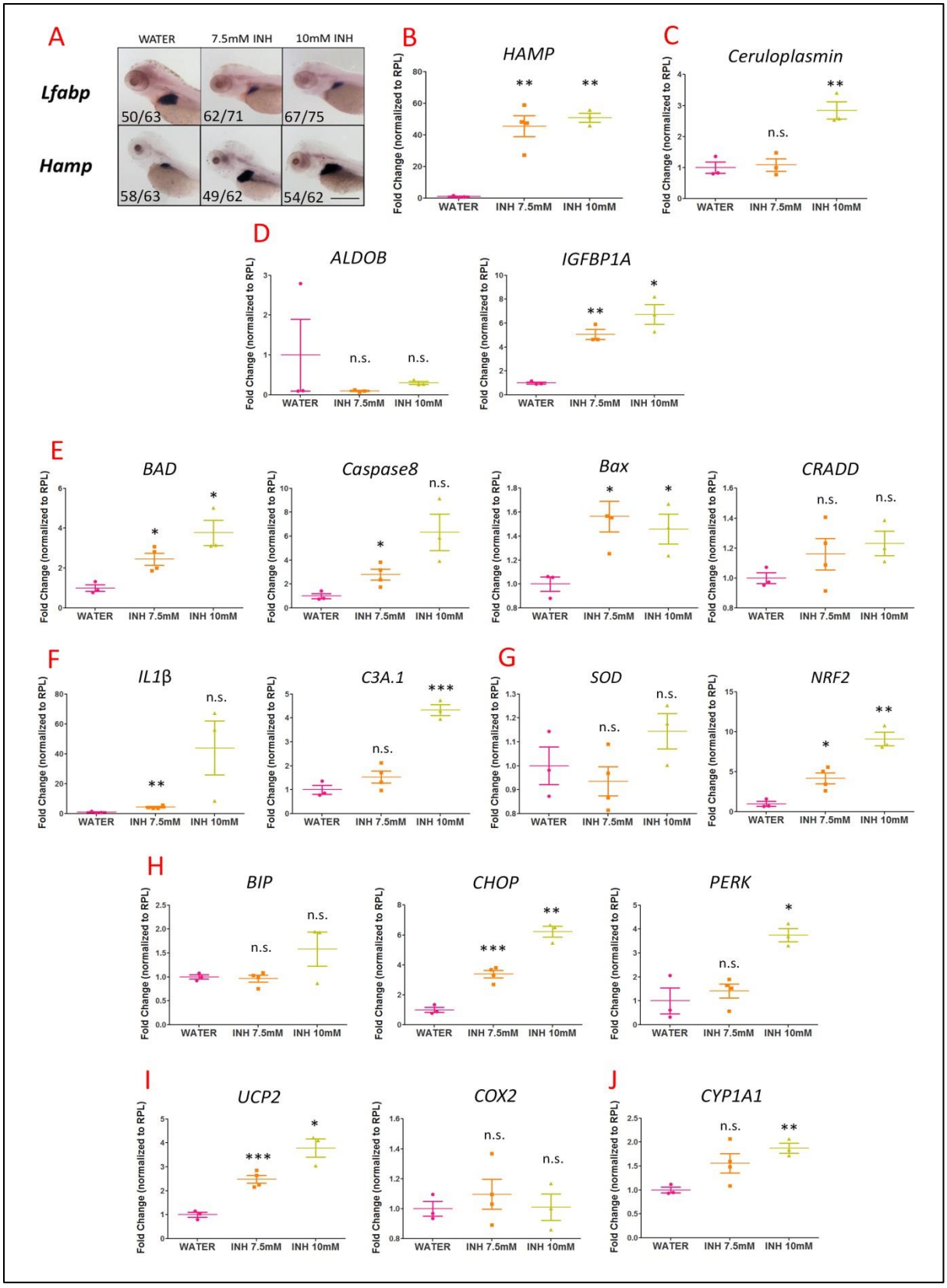

Figure 12: A) *ISH for HAMP (Scale bar: 0.5mm) and* ***B)*** *qRT-PCR for HAMP, shows upregulation in expression for both INH concentrations. Other liver specific genes were tested like* ***C)*** *Ceruloplasmin,* ***D)*** *Aldolase b (aldob) and IGFBP1A.* ***E)*** *Apoptosis markers like Caspase8, BAD, BAX and CRADD, Inflammation markers like F)* *IL1β and C3A.1,* ***G)*** *ROS markers SOD and NRF2, ER stress markers*

like ***H)*** *BIP, CHOP and PERK, mitochondrial stress markers* ***I)*** *UCP2 and COX2 and J****)*** *drug metabolism marker CYP1A1, were also tested. Y-axis: Fold change normalized to RPL. Please note that all qRT-PCR's have to be repeated.*

3.3 DEVELOPMENTAL DEFECTS AND REGENERATION POST DRUG DAMAGE

As mentioned earlier, based on the survival study, we chose concentrations which were not lethal but caused liver damage. Next, we analysed post damage effects on the embryos. After removing the treatment, embryos were transferred into 6-well plates (10-15 embryos per well) and developmental defects were observed over the next 5 days i.e. 0 to 4 days post damage (DPD),

3.3.1 Post-APAP developmental defects

The following defects were observed in APAP treated embryos–

1. Pericardial Oedema
2. Yolk sac oedema
3. Uninflated swim bladder
4. Bent body axis
5. Cartilage defects (beak phenotype in place of jaw)

Survival graph indicates increased death of APAP treated embryos at 3DPD (Fig 13A), with 17.5mM being more fatal than 15mM APAP concentration. All APAP treated embryos show development of pericardial oedema (Fig 13B) and uninflated swim bladder (Fig 13C) by 1DPD. These phenotypes grew more severe with time. By 2DPD, many of these embryos developed yolk sac oedema (Fig 13D). Based on these phenotypes, embryos were divided into mild and severe categories (Fig 13E) APAP toxicity even after its removal can be clearly seen from Fig 13F. Figure 13F shows the distribution of all 3 phenotypes for 15mM and 17.5mM APAP from 0DPD to 2DPD. Embryos suffering from severe malformations do not survive by 3/4DPD and is reflected in the higher death rate from 3DPD (Fig 13A).

We have also tested for regeneration post APAP damage using ISH as well as fluorescent imaging. This proved to be quite challenging for APAP damage as most of the embryos developed pericardial oedema which did not allow proper fluorescent visualization of the embryos or even staining. An alternative would be to do a qRT-

PCR for all stages from 0-4DPD and check for *fabp10a* levels. But, due to lack of time, we have been unable to do so.

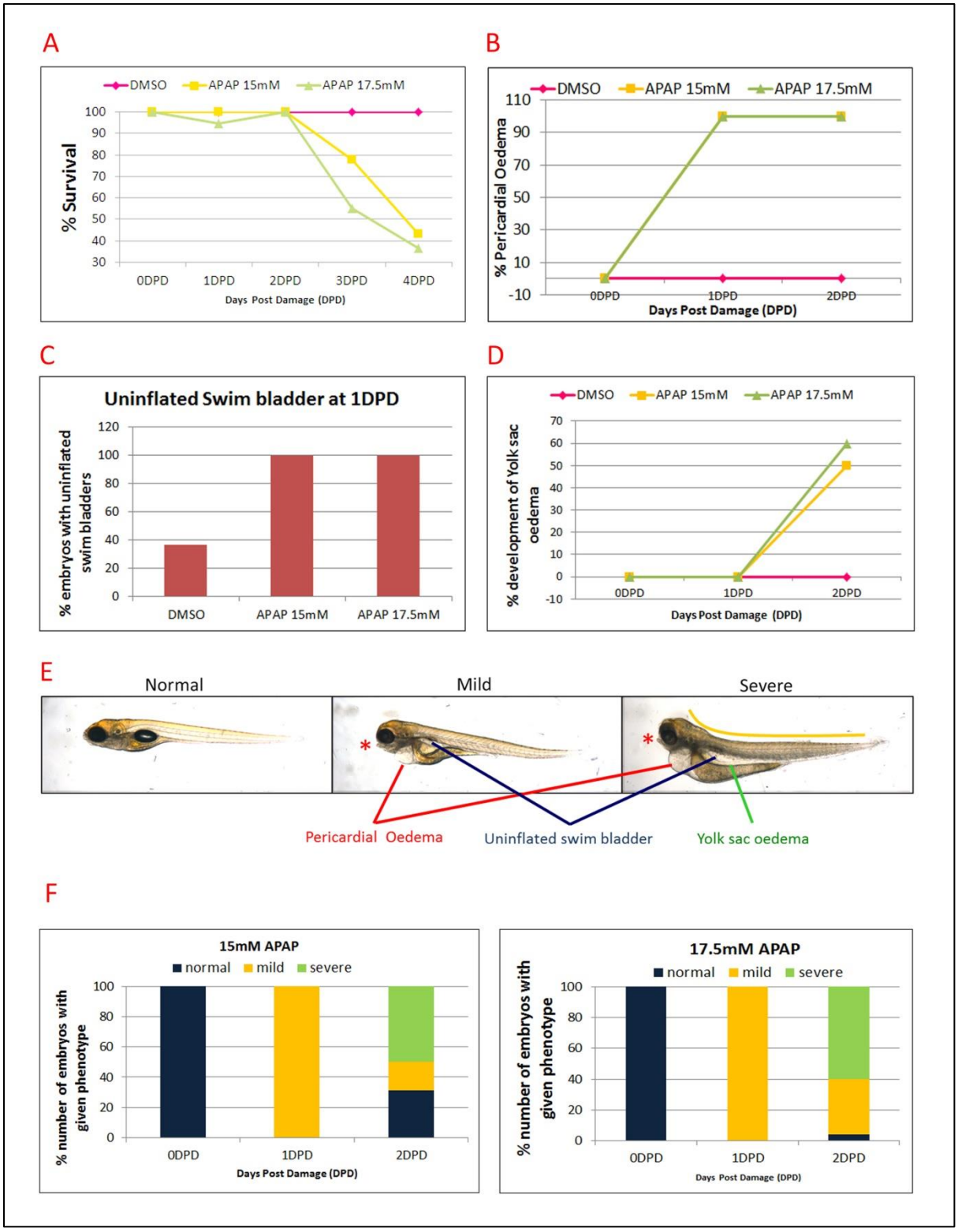

Figure 13: A) *Survival graph of embryos post damage with APAP. Death rate for 17.5Mm APAP is more severe.* ***B)*** *Both concentrations of APAP have 100% development of pericardial oedema.* ***C)*** *All embryos show uninflated swim bladders by 1DPD post APAP treatment.* ***D)*** *Developmental rate of*

yolk sac oedema formation post APAP treatment. ***E)*** *Figure depicts the different types of phenotypes formed and the different categories of "mild" and "severe". Note that the (*) indicates beak-like phenotype and the orange arc indicates bent body axis.* ***F)*** *The percentage number of embryos having "mild" and "severe" phenotypic conditions from 0-2DPD.*

3.3.2 Developmental defects and regeneration of INH

The defects observed in INH treated embryos were found to be similar to APAP treated embryos and are given as follows –

1. Pericardial Oedema
2. Yolk sac oedema
3. Uninflated swim bladder
4. Bent body axis
5. Cartilage defects (beak phenotype in place of jaw)
6. Tail defects – cricked and bent tails

Like APAP, INH treated embryos showed reduced survival post 2DPD (Fig 14A). By 1DPD, all embryos developed uninflated swim bladder (Fig 14C) with many of them showing beak-like phenotypes (Fig 14B). However, unlike APAP treatment, the rate pericardial/yolk-sac oedema formation is not as high. Phenotypically, many of the treated embryos are comparable to the untreated ones (Fig 14F). All the defects in embryos (Fig 14D and Fig 14E) were sorted into mild and severe (Fig 14E) categories. Quantification on the visual basis of these phenotypes is given in Fig 14F. Many embryos developed "mild" defects by 1DPD but were rescued by 2DPD. The development of "severe" characteristics, however, increases by 2DPD. When compared to APAP, the development of "mild" phenotype was much less severe in INH damage at 1DPD (100% in APAP v/s 20% in INH).

In order to check for liver's ability to regenerate following INH-induced damage, we tested for liver size by fluorescence (in the transgenic mentioned above) and by RNA-ISH of *fabp10a* in a temporal manner after termination of INH treatment. All the survived embryos were able to naturally regenerate the liver (image not shown). The same has yet to be confirmed by qRT-PCR of liver specific genes.

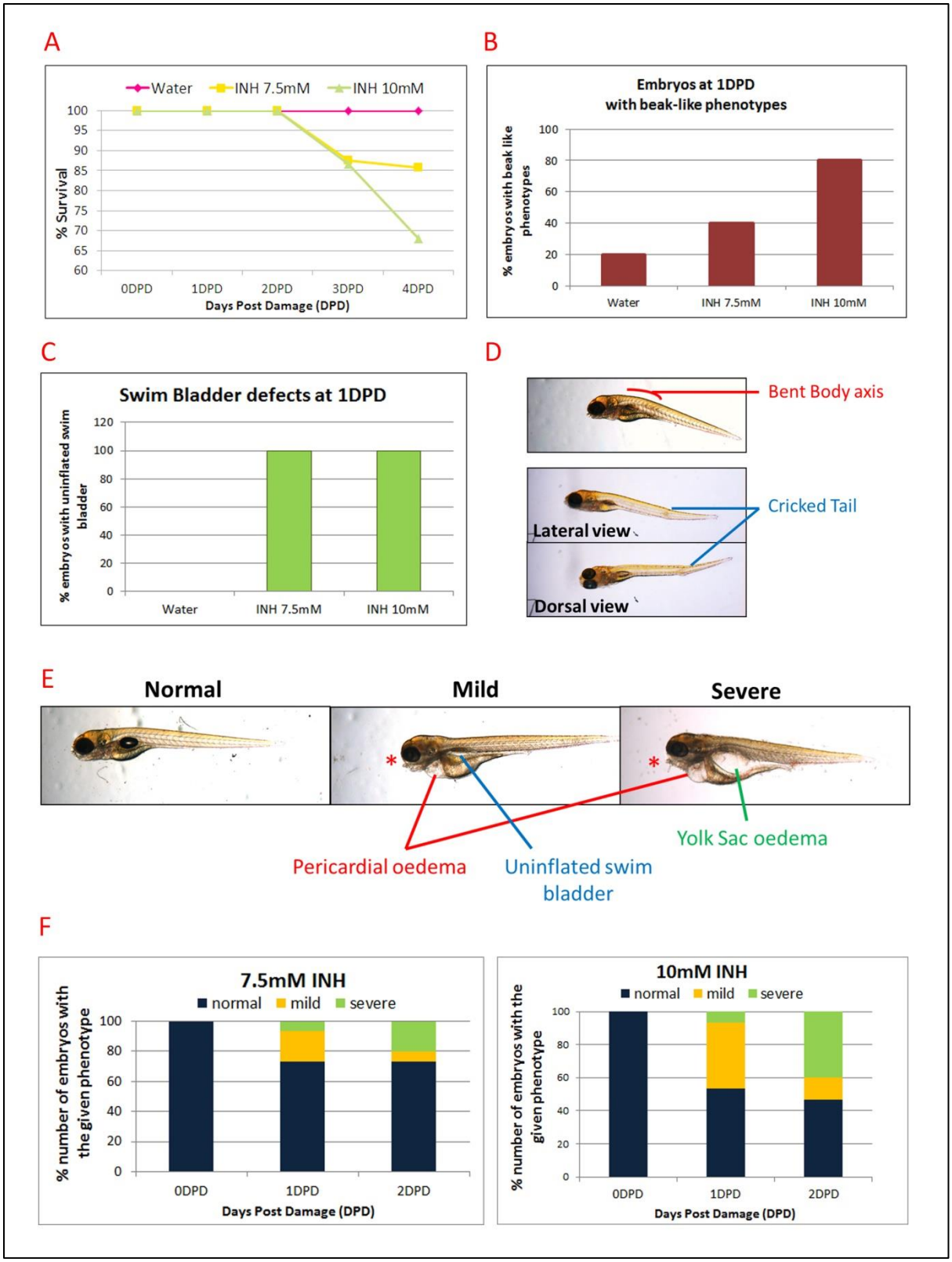

Figure 14: A) *Survival graph of embryos post damage with INH Death rate for 10mM INH is more severe.* ***B)*** *Development rate of beak-like phenotype post damage.* ***C)*** *All embryos show uninflated swim bladders by 1DPD post INH treatment. There are 0 embryos having uninflated swim bladders in Water control.* ***D)*** *Bent body axis and cricked/bent tail defects post INH treatment.* ***E)*** *Figure depicts*

the other different types of phenotypes formed and the different categories of "mild" and "severe". Note that the (*) indicates beak-like phenotype. ***F)*** *The percentage number of embryos having "normal", "mild" and "severe" phenotypic conditions from 0-2DPD in 7.5mM and 10mM INH treatment.*

3.4 SMALL MOLECULE SCREENING FOR ANTIDOTES OF LIVER DAMAGE

Using the standardized model of INH, we performed a small molecule screening for drugs which could potentially revert/protect against Isoniazid induced hepatotoxicity. Using the standardized assay of INH-toxicity, embryos were co-treated with INH 7.5mM and the 15 selected drugs (10µM concentration was used for all drugs for Initial screening). RNA in-situ hybridization of *fabp10a* served as readout. Out of 15 drugs tested, we identified CSLR001[#] to significantly rescue INH-induced liver damage (Fig 15B). Addition of CSLR001 (1.25µM and 2.5µM) to undamaged embryos also leads to significant increase in liver size as observed after RNA-ISH with *fabp10a*. Figure 15A depicts the in-situ hybridization quantification. This potency will further be checked in an increased INH-concentration background i.e. 10mM. It is also worth checking if CSLR001 can show protection even in APAP-induced liver toxicity. For INH, further experiments in order to elucidate the mechanism of CSLR001 are required.

[#] The name of the molecule coded at CSIR-IGIB

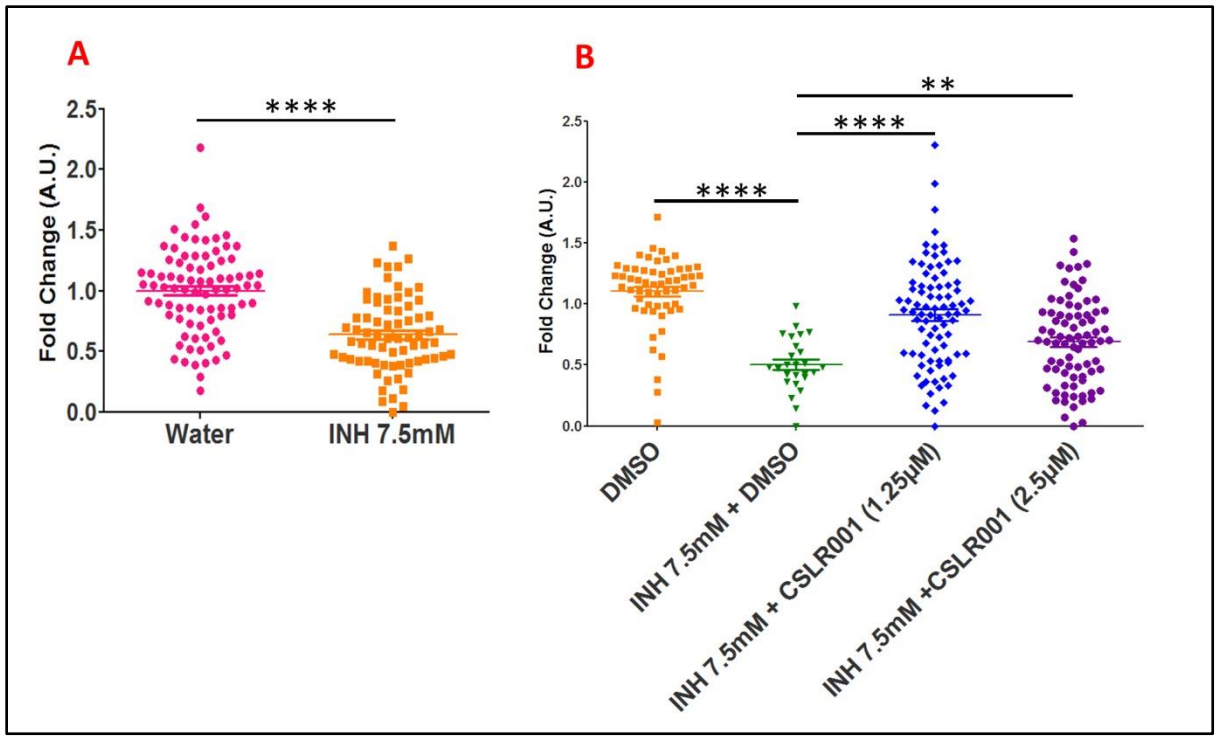

Figure 15: A) *In-situ hybridization quantification (fabp10a) of embryos treated with INH 7.5mM showing significant decrease in liver size when compared to the water control.* ***B)*** *In-situ hybridization quantification (fabp10a) of embryos co-treated with INH 7.5mM and CSLR001 (1.25µM and 2.5µM). Co-treatment with CSLR001 shows induction in fabp10a when compared to INH 7.5mM+DMSO treated embryos.*

4. DISCUSSION

Over the last century, with the advent of technology, the number of medicinal drugs has increased exponentially. The upcoming drugs however, come along with side-effects. One of the very common side-effect is liver injury. In the past, many drugs which pass the clinical trial have not been checked for their effects on liver and many among the ones which have been tested have shown to have a derogatory effect on liver structure and function. As a result of awareness, many drugs are under scrutiny for their hepatotoxic side-effects. Although liver has the capacity to regenerate, under conditions of toxic insults such as drug overdose, this ability fails to overcome the damage. This has increasingly become a serious health concern and currently we do not have any counter measures to help the same. There is a need for therapeutics that may protect/promote liver regeneration in the background of DILI. In this study, our interest is to screen for potential small molecules which may

provide protection in DILI background. For that purpose, we developed Acetaminophen and Isoniazid-induced liver damage models in Zebrafish and screened for molecules in the same.

Acetaminophen, commonly known as Paracetamol is widely used as an antipyretic and anti-analgesic. It is one of the biggest contributors to DILI. Hepatotoxicity of this molecule has been widely studied and standardized damage models have been developed in mice as well as zebrafish (North et al., 2010; Weigt et al., 2010). We utilized zebrafish as a model system for its advantage of offering drug-screening in vivo. Upon standardization, 15mM and 17.5mM APAP were found to be sufficient to cause liver damage without any abnormal phenotype. We used *fabp10a*, a previously established marker of liver size as readout. RNA-ISH as well as qRT-PCR showed decrease in transcript levels of this gene signifying affected liver size. Contrary to *fabp10a*, another liver specific marker *HAMP* showed significant upregulation. *HAMP* upregulation has been linked to increased inflammation and it is also known that liver damage by APAP leads to increased inflammation (Blazka et al., 1995; D'Angelo, 2013; Krenkel et al., 2014; Zhao et al., 2013). This might be the reasoning behind the increased transcript levels of *HAMP*. Other liver specific genes such as *IGFBP1a* and *ceruloplasmin* were also found to be upregulated, the explanation for which is still not known. Increased expression of cell death markers clearly suggests the apoptosis induced by APAP treatment. Increased ROS might be the cause of apoptosis and therefore liver damage. However, confirmatory experiments are needed.

INH is a front-line antimicrobial for tuberculosis since many decades. However, it has been shown to cause hepatotoxicity in various vertebrate models including humans (Ahadpour et al., 2015; Black et al., 1975; Boelsterli and Lee, 2014; Hassan et al., 2015; Metushi et al., 2016; Wang et al., 2016). There are very few studies which have shown hepatotoxicity of INH in zebrafish (Anju et al., 2016; Zhang et al., 2014). Studies also have shown that genetic predisposition to N-Acetyltransferase 2 (NAT2) polymorphisms play a key role and are essential for INH induced liver toxicity. They have suggested that slow acetylators have a greater chance of INH-induced hepatitis (Huang et al., 2002; Lee et al., 2010; Zabost et al., 2013). Therefore, due to such contradictory statements, the hepatotoxicity of INH is still an open question. With our study, we suggest that even without genetic predisposition, INH by itself is sufficient

to cause hepatotoxicity. Using Zebrafish model, 7.5mM and 10mM INH after the course of 24 hours caused significant reduction in liver size. Like APAP, INH treatment also showed increase in *HAMP* and other liver specific genes. DCFDA assay showed increase in ROS levels. Similarly, increased expressed in apoptosis markers (*caspase, BAD, BAX, CRADD*) suggests increased cell death post damage. As suggested that increased *HAMP* expression could be a possible result of inflammation, we tested the status of inflammatory markers and found high upregulation of *IL-1β*. We also tested for *C3a.1*. *C3a* in humans is a part of the complement system and also plays a role in immunity (Klos et al., 2009). Increased *C3a* expression has also been linked to inflammation as well as liver regeneration post injury (Markiewski et al., 2010; Strey et al., 2003). Its zebrafish ortholog *C3A.1* transcript levels were induced post-INH damage. It is possible that it might be a result of system's attempt of overcoming the damage and prepping for regeneration. As a probable outcome of inflammation, we found a significant upregulation in genes involved in detoxification suggesting that cells might be trying to cope with the insult. *CYP1a1*, which is involved in drug metabolism (Walsh et al., 2013; Zanger and Schwab, 2013), is also upregulated. At the organelle level, the status of mitochondria and ER was checked. In case of mitochondrial markers, *UCP2* is upregulated and *COX2* is not changing at all. In case of ER stress markers, again *CHOP* and *PERK* are upregulated. This suggests that perhaps INH may cause both ER and mitochondrial stress thereby causing cytotoxicity.

From this study, we show that Acetaminophen and Isoniazid might be hepatotoxic. However, in depth studies with confirmatory experiments to conclusively prove the same are necessary. In embryos it can be shown by multiple ways such as whole mount tunel assay, FACS based isolation of fluorescent hepatocytes and propidium iodide staining to distinguish between live and dead cells, apoptag staining etc. Another important alternative is to demonstrate the tissue damage in adult fish. Liver can be dissected and sectioned easily and observed for altered morphology, if any, by a well standardized H&E staining. By observing the H&E staining for both the drugs, it is evident that they cause morphological changes to the liver. This damage to the tissue can be correlated to distorted morphology and increased intercellular spaces in drug treated adult zebrafish livers.

Using the INH damage model, we were also able to screen 15 drugs and identified CSLR001 as a potential rescuer of liver toxicity. Further experiments towards its mechanism as a hepatoprotective molecule are much needed and will be addressed in our future studies

In conclusion, we have successfully developed 2 DILI models of acetaminophen and Isoniazid in zebrafish. We were able to standardize the concentration for both the hepatotoxic drugs in embryonic as well as adult zebrafish and assess the level of damage by measuring the decrease in *fabp10a* by multiple methods. We were further able to characterise to some extent the damage by using techniques like DCFDA and qRT-PCR. INH damage model was used to screen for hepatoprotective agents and we have identified one such molecule. Now these models can be used to further study their mechanism of action. This will enable us to get a better insight in liver biology and the mechanism of regeneration, thus enabling us to develop far more efficient assays and therapeutics against Drug-induced Liver Injury.

5. REFERENCES -

Ahadpour, M., Eskandari, M.R., Mashayekhi, V., Haj, K., Ebrahim, M., Jafarian, I., and Hosseini, M. (2015). Mitochondrial oxidative stress and dysfunction induced by isoniazid : study on isolated rat liver and brain mitochondria study on isolated rat liver and brain mitochondria. Drug and Chemical Toxicology.

Almazroo, O.A., Miah, M.K., and Venkataramanan, R. (2017). Drug Metabolism in the Liver. Clinics in Liver Disease *21*, 1–20.

Anju, T., Preetha, R., Shunmugam, R., Mane, S.R., Arockiaraj, J., and Kumaresan, V. (2016). Norbornene derived nanocarrier reduces isoniazid mediated liver toxicity: assessment in HepG2 cell line and zebrafish model. RSC Advances *6*, 114927–114936.

Atkuri, K.R., Mantovani, J.J., Herzenberg, L.A., and Herzenberg, L.A. (2007). N - Acetylcysteine — a safe antidote for cysteine / glutathione deficiency. Current Opinion in Pharmacology *7*, 355–359.

Au, J.S., Navarro, V.J., and Rossi, S. (2011). Review article: Drug-induced liver

injury - Its pathophysiology and evolving diagnostic tools. Alimentary Pharmacology and Therapeutics *34*, 11–20.

Bessone, F. (2010). Non-steroidal anti-inflammatory drugs : What is the actual risk of liver damage ? World J. Gastroenterol. *16*, 5651–5661.

Black, M., Mitchell, J.R., Zimmerman, H.J., Ishak, K.G., and Epler, G.R. (1975). Isoniazid-associated hepatitis in 114 patients. Gastroenterology *69*, 289–302.

Blazka, M.E., Wilmer, J.L., Holladay, S.D., Wilson, R.E., and Luster, Michael, I. (1995). Role of Proinflammatory cytokines in Acetaminophen Hepatotoxicity. Toxicology and Applied Pharmacology *133*, 43–52.

Boelsterli, U.A., and Lee, K.K. (2014). Mechanisms of isoniazid-induced idiosyncratic liver injury : Emerging role of mitochondrial stress. Journal of Gastroenterology and Hepatology *29*, 678–687.

Corsini, A., and Bortolini, M. (2013). Drug-Induced Liver Injury: The Role of Drug Metabolism and Transport. Journal of Clinical Pharmacology *53*, 463–474.

D'Angelo, G. (2013). Role of Hepcidin in the pathophysiology and diagnosis of anemia. Blood Research *48*, 10–15.

Fausto, N., Laird, a D., and Webber, E.M. (1995). Role of growth regeneration factors and cytokines in hepatic. FASEB Journal *9*, 1527–1536.

Forget, E.J., and Menzies, D. (2006). Adverse reactions to first-line antituberculosis drugs. 231–249.

Hassan, H.M., Guo, H.L., Yousef, B.A., Luyong, Z., and Zhenzhou, J. (2015). Hepatotoxicity mechanisms of isoniazid: A mini-review. Journal of Applied Toxicology *35*, 1427–1432.

Heard, K.J. (2009). Acetylcysteine for Acetaminophen Poisoning Kennon. N Engl J Med *359*, 285–292.

Hong, C., and Tontonoz, P. (2014). Liver X receptors in lipid metabolism: opportunities for drug discovery. Nature Reviews. Drug Discovery *13*, 433–444.

Huang, Y., Chern, H., Su, W., Wu, J., Lai, S., Yang, S., Chang, F., and Lee, S. (2002). Polymorphism of the N-Acetyltransferase 2 Gene as a Susceptibility Risk Factor for Antituberculosis Drug–Induced Hepatitis. Hepatology *35*, 883–889.

Kamalakkannan, N., Rukkumani, R., Aruna, K., Varma, P., Viswanathan, P., and Menon, V. (2005). Protective Effect of N-Acetyl Cysteine in Carbon Tetrachloride-Induced Hepatotoxicity in Rats. Iranian Jounal of Pharmacology and Therapeutics *4*, 118–123.

Klos, A., Tenner, A.J., Johswich, K., Ager, R.R., Reis, E.S., and Köhl, J. (2009). The role of the anaphylatoxins in health and disease. Molecular Immunology *46*, 2753–2766.

Ko, U.A., Speicher, T., and Werner, S. (2010a). Regulation of liver regeneration by growth factors and cytokines. EMBO Molecular Medicine *2*, 294–305.

Ko, U.A., Speicher, T., and Werner, S. (2010b). Regulation of liver regeneration by growth factors and cytokines. 294–305.

Krenkel, O., Mossanen, J.C., and Tacke, F. (2014). Immune mechanisms in acetaminophen-induced acute liver failure. Hepatobiliary Surgery and Nutrition *3*, 331–343.

Larson, A.M., Polson, J., Fontana, R.J., Davern, T.J., Lalani, E., Hynan, L.S., Reisch, J.S., Schiødt, F. V, Ostapowicz, G., Shakil, A.O., et al. (2005). Acetaminophen-induced Acute Liver Failure: Results of the United States Multicenter, Prospective study. Hepatology *42*, 1364–1372.

Lee, S., Chung, L.S., Huang, H., Chuang, T., Liou, Y., and Wu, L.S. (2010). NAT2 and CYP2E1 polymorphisms and susceptibility to fi rst-line anti-tuberculosis drug-induced hepatitis. The International Journal of Tuberculosis and Lung Disease *14*, 622–626.

Liver Disease in India Liver Disease in India.

Lu, Z., Bourdi, M., Li, J.H., Aponte, A.M., Chen, Y., Lombard, D.B., Gucek, M., Pohl, L.R., and Sack, M.N. (2011). SIRT3-dependent deacetylation exacerbates acetaminophen hepatotoxicity. EMBO Reports *12*, 840–846.

Mahadevan, S.B.K., Mckiernan, P.J., Davies, P., and Kelly, D.A. (2006). Paracetamol induced hepatotoxicity. *91*, 598–603.

Markiewski, M.M., DeAngelis, R.A., Chrishtoph, S.W., Foukas, P.G., Gerard, C., Gerard, N., Wetsel, R.A., and Lambris, J.D. (2010). The Regulation of Liver Cell Survival by Complement. Journal of Immunologu *182*, 5412–5418.

Metushi, I., Uetrecht, J., and Phillips, E. (2016). Mechanism of isoniazid-induced hepatotoxicity : then and now. British Journal of Clinical Pharmacology *81*, 1030–1036.

Michalopoulos, G.K. (1990). Liver regeneration: molecular mechanisms of growth control. FASEB Journal *4*, 176–187.

Navarro, V.J., and Senior, J.R. (2006). Drug-Related Hepatotoxicity. The New England Journal of Medicine *354*, 731–739.

Nguyen, P., Leray, V., Diez, M., Serisier, S., Le Bloc'H, J., Siliart, B., and Dumon, H. (2008). Liver lipid metabolism. Journal of Animal Physiology and Animal Nutrition *92*, 272–283.

North, T.E., Babu, I.R., Vedder, L.M., Lord, A.M., Wishnok, J.S., Tannenbaum, S.R., Zon, L.I., and Goessling, W. (2010). PGE2-regulated wnt signaling and N-acetylcysteine are synergistically hepatoprotective in zebrafish acetaminophen injury. Proceedings of the National Academy of Sciences *107*, 17315–17320.

Pellicoro, A., Ramachandran, P., Iredale, J.P., and Fallowfield, J.A. (2014). Liver fibrosis and repair: immune regulation of wound healing in a solid organ. Nat Rev Immunol *14*, 181–194.

Rui, L. (2014). Energy metabolism in the Liver. Comprehensive Physiology *4*, 177–197.

Russmann, S., Kullak-Ublick, G.A., and Grattagliano, I. (2009). Current Concepts of Mechanisms in Drug-Induced Hepatotoxicity. Current Medicinal Chemistry *16*, 3041–3053.

Ryder, S.D., and Beckingham, I.J. (2001). Other causes of parenchymal liver disease. British Medical Journal (Clinical Research Ed.) *322*, 290–292.

Strey, C.W., Markiewski, M., Mastellos, D., Tudoran, R., Spruce, L.A., Greenbaum, L.E., and Lambris, J.D. (2003). The Proinflammatory Mediators C3a and C5a Are Essential for Liver Regeneration. The Journal of Experimental Medicine *198*, 913–923.

Suk, K.T., Kim, D.J., Kim, C.H., Park, S.H., Yoon, J.H., Kim, Y.S., Baik, G.H., Kim, J.B., Kweon, Y.O., Kim, B.I., et al. (2012). A Prospective Nationwide Study of Drug-Induced Liver Injury in Korea. The American Journal of Gastroenterology *107*, 1380–1387.

The International Liver Congress (2016). Fast facts about liver disease.

The liver - Canadian Cancer Society http://www.cancer.ca/en/cancer-information/cancer-type/liver/liver-cancer/the-liver/?region=on.

Tostmann, A., Boeree, M.J., Aarnoutse, R.E., Lange, W.C.M. De, Ven, A.J.A.M. Van Der, and Dekhuijzen, R. (2008). Antituberculosis drug-induced hepatotoxicity: Concise up-to-date review. Journal of Gastroenterology and Hepatology *23*, 192–202.

Vliegenthart, A.D.B., Tucker, C.S., Del Pozo, J., and Dear, J.W. (2014). Zebrafish as model organisms for studying drug-induced liver injury. British Journal of Clinical

Pharmacology *78*, 1217–1227.

Walsh, A.A., Szklarz, G.D., and Scott, E.E. (2013). Human CYP1A1 Structure and Use in Understanding Metabolism. Journal of Biological Chemistry 1–26.

Wang, P., Pradhan, K., Zhong, X., and Ma, X. (2016). Isoniazid metabolism and hepatotoxicity. Acta Pharmaceutica Sinica B *6*, 384–392.

Weigt, S., Huebler, N., Braunbeck, T., von Landenberg, F., and Broschard, T.H. (2010). Zebrafish teratogenicity test with metabolic activation (mDarT): Effects of phase I activation of acetaminophen on zebrafish Danio rerio embryos. Toxicology *275*, 36–49.

William M, L. (2003). Drug-Induced Hepatotoxicity. The New England Journal of Medicine *349*, 474–485.

Yuan, L., and Kaplowitz, N. (2013). Mechanisms of Drug-Induced Liver Injury. Clinics in Liver Disease *17*, 507–518.

Zabost, A., N, S.B., N, M.K., Maria, B.B., N, J.J., Zwolska, Z., and T, E.A. (2013). Correlation of N-Acetyltransferase 2 Genotype with Isoniazid Acetylation in Polish Tuberculosis Patients. BioMed Research International.

Zanger, U.M., and Schwab, M. (2013). Cytochrome P450 enzymes in drug metabolism : Regulation of gene expression , enzyme activities , and impact of genetic variation. Pharmacology and Therapeutics *138*, 103–141.

Zhang, X., Li, C., and Gong, Z. (2014). Development of a convenient in vivo hepatotoxin assay using a transgenic zebrafish line with liver-specific dsred expression. PLoS ONE *9*.

Zhao, N., Zhang, A.-S., and Enns, C.A. (2013). Iron Regulation By Hepcidin. Science in Medicine *123*, 2337–2343.